Surficial Sediments

Matthew Poti[1,2,3], Brian Kinlan[1,2], and Charles Menza[2]

3.1. SUMMARY

Mapping seafloor features, including sediment characteristics and distribution, provides crucial information for a number of coastal and marine spatial planning applications. Seafloor maps can be used to help identify critical habitat areas for benthic organisms (e.g., clams, corals, demersal fish), select appropriate offshore construction sites, and plan sand/gravel mining operations.

Predictive models of mean grain size, sediment composition, and hard bottom occurrence were developed for the New York study area (Figure 1.2). These new models build upon the data compilations and analytical frameworks laid out by Goff et al. (2008), Poppe et al. (2005) and Greene et al. (2010), respectively. For mean grain size and sediment composition, the models provide continuous, gridded spatially-explicit prediction surfaces and corresponding uncertainty estimates. The hard bottom occurrence model also provides a continuous gridded prediction surface representing the likelihood of hard bottom occurrence. All information was mapped on the same 30 arc-second horizontal resolution grid used to characterize ocean habitat and seabird variables in Chapters 4 and 5 of this report.

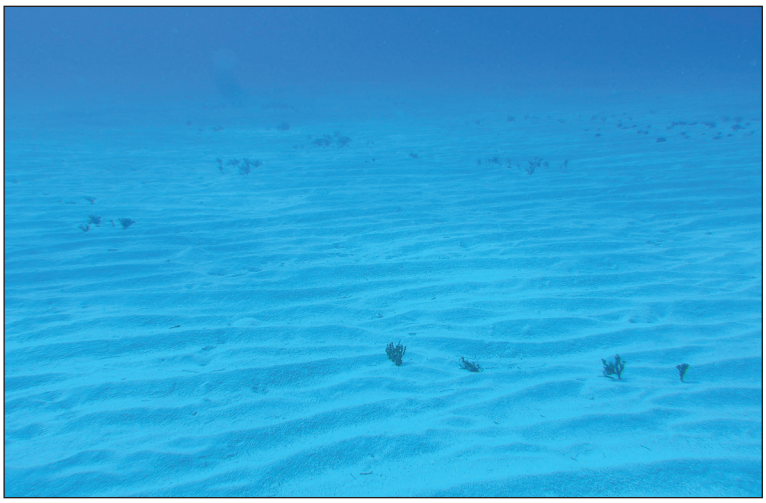

Image 3.1. Example of sand waves. Photo credit: NOAA/CCMA/ Biogeography Branch.

3.2. BACKGROUND

The New York study area, like other broad continental shelf regions in the northeastern United States, is characterized by spatially variable seafloor features that have formed as a result of dynamic marine geological processes, particularly the dramatic (>100 m) rise in sea level following the last glaciation (Williams et al., 2006; Goff et al., 2008). The present distribution of surficial sediments in the region reflects deposition, erosion, and other sedimentological processes during this period of sea level rise (Williams et al., 2006).

The continental shelf within the study area has relatively simple topography and slopes gently from the shore to the shelf edge 100-150 km from shore (Allen et al., 1983). The seafloor on the continental shelf is composed mostly of sand which grades to silt and clay in deeper areas (Poppe et al., 1994). The relatively homogeneous seafloor is interrupted by sporadic relic sand and gravel ridges, exposed sandstone and bedrock, dumping sites, dredge disposal sites, and artificial reefs (e.g., shipwrecks, lost cargo, submerged pipelines). The most pronounced topographic features in the study area are the Hudson Shelf Valley, which crosses the entire shelf at the southern end of the study area (Butman et al., 2003), and many shelf edge incisions made by submarine canyons. The Hudson Canyon connects to the Hudson Shelf Valley and is the largest submarine canyon on the U.S. Atlantic continental margin (Butman et al., 2006).

Mapping seafloor sediment characteristics is challenging, in part, because of the high variability of sediment characteristics at relatively short spatial scales. Characterization of physical features of the seafloor is often limited by the availability of comprehensive sampling across a wide range of spatial scales (Goff et al., 2008). Traditional bottom grab, core, trawl and camera surveys are limited in their spatial coverage. One solution to this

[1] Consolidated Safety Services, Inc., under NOAA Contract No. DG133C07NC0616
[2] Biogeography Branch, Center for Coastal Monitoring and Assessment, National Centers for Coastal Ocean Science, National Ocean Service, National Oceanic and Atmospheric Administration
[3] Corresponding author: Matthew.Poti@noaa.gov

problem developed in recent decades is the use of acoustic backscatter information to characterize physical properties of seafloor sediments (e.g., Lathrop et al., 2006; De Falco et al., 2010; Harris and Stokesbury, 2010; Brown et al., 2011).

Multibeam and sidescan sonar surveys completed in the New York study area (see Figure 2.1) recorded acoustic backscatter or reflectance data. If appropriately processed, this information can provide fine-scale sediment composition maps in areas of coverage. Acoustic backscatter data is not, however, uniformly available across the NY study area. Moreover, Goff et al. (2008) stressed geographic variability in the relationship between acoustic backscatter and sediment characteristics owing to differences in environmental factors like bathymetric slope and water column properties. They suggested that extensive direct sampling of surficial sediments is needed to assess the correlation between backscatter intensity and sediment character from region to region, which limits its utility to densely ground-truthed areas.

An alternative method is to statistically model the spatial distribution of sediment using large databases assembled from many surveys. Goff et al. (2008) proposed and illustrated this method using the recently compiled U.S. Geological Survey (USGS) Atlantic Coast usSEABED database (Reid et al., 2005). The usSEABED database provides an extensive and heterogeneous collection of seabed survey data derived from a number of sources. The database includes both “extracted” information derived from analytical measurements and “parsed” information that is inferred from word-based descriptions (Reid et al., 2005). Goff et al. (2008) found that usSEABED parsed and extracted mean grain size data were suitable for use in sediment mapping even though data were collected using a range of methodologies across several decades, provided they were appropriately quality-controlled and bias-corrected. The predictive models described in this chapter are built on quality-controlled and bias-corrected usSEABED data.

Two notable additional mapping efforts have produced sediment grain size distribution maps for the U.S. Atlantic coast. First, the USGS Continental Margin Mapping (CONMAP) Program developed a coarse-scale sediment grain size distribution map for the U.S. East Coast continental margin through the analysis and compilation of thousands of sediment samples, many of which are part of usSEABED. The CONMAP sediment data layer is a vector dataset with polygons classified according to the dominant surficial sediment type (Poppe et al., 2005). The metadata provided with the CONMAP sediment data layer indicates that this dataset does not capture localized features of sediment distribution and should be used mainly to describe regional trends in sediment grain size distribution (Poppe et al., 2005). It is therefore useful mainly as a qualitative mapping aid. Second, as part of the Northwest Atlantic Marine Ecoregional Assessment, The Nature Conservancy (TNC) produced a map of soft sediment characteristics using an interpolation of mean grain size point data from the usSEABED sediment database (Greene et al., 2010). A point dataset of hard bottom locations derived from the usSEABED dataset and National Marine Fisheries Service (NMFS) bottom trawl survey data was overlaid on the soft sediment map to identify hard bottom areas (Greene et al., 2010). The TNC maps were aimed at broad scale regional planning and did not provide a spatial assessment of map accuracy.

The present study aims to build on previous mapping efforts by developing maps more appropriate for fine scale planning decisions in the NY study area, with spatially explicit accuracy maps.

3.3. METHODS

3.3.1. Study Region and Grid

Predictions for mean grain size, sediment composition and the likelihood of hard bottom occurrence were made on a 30 arc-second spatial resolution geographic grid spanning the New York study area. The same grid was applied to predict oceanographic variables (Chapter 4) and seabird distributions (Chapter 6). The 30 arc-second grid has a north-south linear dimension of 0.927 km and an average east-west linear dimension of 0.814 km in the study area. For simplicity, decimal degrees were used to keep track of grid cell centroids and measure distances using a simple elliptical geodetic approximation; the effects of this simplifying assumption were negligible given the size of our study region and grid configuration (potential errors in linear distances < 50% of grid cell horizontal resolution).

3.3.2. Mean Grain Size

Data Preparation

We obtained the quality-controlled, bias-corrected, merged parsed and extracted database of mean sediment grain size (φ) described in Goff et al. (2008) from the lead author of that study (Dr. John Goff, University of Texas at Austin). Mean grain size is reported in φ units, where $\varphi = -\log_2$(mean grain diameter in mm) (Krumbein and Sloss 1963). In this scale, gravel corresponds to -6 to -1 φ, sand corresponds to -1 to 4 φ, and mud corresponds to 4 to 12 φ.

Goff's dataset was derived from the publicly available usSEABED Atlantic Coast Offshore Surficial Sediment Data Release, version 1.0 (Reid et al., 2005). The original usSEABED extracted and parsed datasets were filtered to remove records that did not relate to surficial sediments. At locations with multiple records pertaining to surficial sediments, mean grain size was averaged. Since the laboratory-based analyses used to generate the extracted data may exclude hard components like shell and gravel and may therefore introduce a bias toward finer particles (Williams et al., 2006; Harris and Stokesbury, 2010), the parsed data were bias-corrected as described in Goff et al. (2008) prior to merging the extracted and parsed data. Goff's data covered only the mid-Atlantic portion of the U.S. Atlantic coast. We extracted a subset of the data including the NY study area for further analysis.

Development of the Mean Grain Size Model

A geostatistical modeling approach was used to predict a continuous, gridded surface for surficial sediment mean grain size from scattered sediment survey point data and to generate corresponding spatially-explicit uncertainty estimates. The same general modeling approach used for the bathymetry prediction and described in Section 2.3.1 was used for this analysis and is not reiterated here (see Cressie 1993 and Figure 2.3 for work flow). All geostatistical modeling steps were performed in ArcGIS 10 using the Spatial Analyst and Geostatistical Analyst toolboxes (ESRI 2011a).

The deterministic mean trend was estimated using local polynomial interpolation (LPI), a semi-parametric local regression technique that creates a prediction surface by fitting polynomial functions of a specified degree to data in overlapping search neighborhoods defined by a constant search radius, or bandwidth (ESRI 2011a). LPI uses weighted least-squares regression, with weights equal to 0 outside the search neighborhood, and a Gaussian function of distance inside the search neighborhood. LPI was chosen over other techniques because it provides approximate parametric confidence intervals, and because bandwidth can be adjusted to ensure that only broad-scale trends are captured, leaving more localized information in residuals. LPI outputs are a prediction surface, an approximate parametric prediction standard error surface, indicating the uncertainty associated with the prediction at each location, and a spatial condition number surface, indicating the stability of the local regression model at each location. Higher spatial condition number values indicate that the solution is less stable, such that small variations in the input data (e.g., uncertainty due to measurement error) can result in large variations in the prediction. For second order polynomials, the critical spatial condition number threshold value is 100 (Golub and Van Loan, 1996), meaning that predictions should be considered with caution at locations where the spatial condition number is close to 100 and should be considered unreliable where it is greater than 100. We used second degree (quadratic) polynomials, an eight sector circular search neighborhood with 1 decimal degree bandwidth (~111 km), and Gaussian kernel weights. At least 10 and no more than 250 data from each sector were used to produce each trend prediction. The eight-sector neighborhood search was used to mitigate the effects of uneven sample distribution on the trend surface estimation.

Residuals were obtained by subtracting the trend surface prediction at each data location from the observed data value. Residuals were checked for normality by examining histogram and normal QQ plots. A sample semivariogram of the residuals was then calculated in ArcGIS 10 using the Geostatistical Analyst extension (ESRI, 2011a). Lag size was selected based on examining the distribution of nearest-neighbor distances, choosing the smallest lag size that would allow sufficient samples to estimate semivariance values near the origin. Anisotropy (i.e., changes in spatial autocorrelation due to direction) was checked using directional semivariograms. To model spatial autocorrelation in residuals, a constrained weighted least squares algorithm was used to fit an exponential anisotropic model to the sample semivariogram (model parameters in Table 3.1).

Fitted semivariogram model parameters were used to perform ordinary kriging (OK) of the residuals in ArcGIS 10 using eight-sector search neighborhoods and anisotropic search neighborhood radii equal to the radii of the anisotropic semivariogram model. At least 5 and no more than 25 data points from each sector were used to produce kriging predictions on a 30 arc-second grid. Kriging predictions were generated at the centroid of each grid cell. We confirmed that centroids did not intersect with data point locations, so that the nugget effect (measurement error and small-scale variance) was "filtered out" of the kriging prediction. This resulted in a desirable noise reduction in the prediction surface, equivalent to the maximum a posteriori resampling algorithm used by Goff et al. (2006, 2008).

Table 3.1. Semivariogram parameters for the mean grain size model.

DATA	n	TYPE OF VARIO-GRAM MODEL	NO. OF LAGS	LAG SIZE (km)[b]	NUGGET	MAJOR RANGE (km)[b]	MINOR RANGE (km)[b]	DIREC-TION (°)[c]	PARTIAL SILL	% OF THE SILL DUE TO THE NUGGET
Mean Grain Size[a]	14,612	Exp	50	1.11	1.26	24.44	12.22	288.05	0.98	56.25

a - in φ units, where $\varphi = -\log_2$(mean grain diameter in mm); b - converted from decimal degrees to kilometers using 111.1 km/decimal degree;

c - clockwise from North; Exp = Exponential

The model surface representing the predicted mean grain size was calculated as the sum of the trend (LPI) and residual (kriging) prediction surfaces. The corresponding prediction standard error surface was calculated as the square root of the sum of the trend and kriging prediction variances (errors in the trend and residual surfaces are assumed to be independent). The final prediction and prediction standard error surfaces were exported as ESRI grids with the extent and spatial resolution described in Section 3.3.1. An error mask was applied to the output grids to exclude areas where the kriging standard error was greater than 97.5% of the residual sample standard deviation. This error mask was applied to all surficial sediment outputs for consistency.

In addition to the prediction and prediction standard error maps, a vector dataset with polygons classified by mean grain size classes was generated by assigning each grid cell a mean grain size class using the classification scheme of Wentworth (1922). Finally, the probability of mean grain size exceeding the thresholds 25.6 cm ($\varphi < -8$, boulders and larger), 6.4 cm ($\varphi < -6$, cobbles and larger), 2 mm ($\varphi < -1$, pebbles and larger), and 0.062 mm ($\varphi < 4$, very fine sand and larger) were mapped, by integrating under the normal distribution defined for each grid cell by the OK prediction mean and variance.

3.3.3. Sediment Composition

Data Preparation

Seabed survey data from the usSEABED Atlantic Coast Offshore Surficial Sediment Data Release, version 1.0 (Reid et al., 2005) parsed and extracted databases were used to develop models of the fractional composition of mud, sand, and gravel in surficial sediments in the study area. Data were downloaded from the USGS publications website (http://pubs.usgs.gov/ds/2005/118/htmldocs/usseabed.htm). The dataset provided by Dr. Goff for the mean grain size analysis was not used for sediment composition modeling because it did not include percentages of mud, sand, and gravel. The survey point data was filtered to remove duplicate points and points not relating to surficial sediments. Survey records were removed if the "sample phase" attribute for the database record indicated that the sample was clearly not from surficial sediments (e.g., from the bottom of the sample core). When multiple records referred to the same sample core, the record that described the top of the sample core (as indicated by the "sample top" attribute) was retained and the other records were removed. When multiple records pertaining to surficial sediments existed at a location, values for percent mud, percent sand, and percent gravel were averaged. When the sum of all fractions exceeded 100%, each of the mud, sand, and gravel percentages was divided by the sum to re-normalize sums to 100% (sums were seldom greater than 110% so any error introduced by this re-normalization procedure would be small). Separate datasets for each sediment type were extracted, excluding records with "no data" for the given sediment type (but including 0% values). Percentages were converted to fractional values between 0 and 1 for subsequent processing.

Development of the Sediment Composition Models

The same geostatistical approach used to model mean grain size (see Section 3.3.2) was applied separately to each of the individual sediment type datasets. The deterministic mean trend was fit using the same LPI parameters as described for the mean grain size model in Section 3.3.2. Specific exponential anisotropic models for each sediment type were fitted to the sample semivariogram as described in Section 3.3.2 (model parameters are shown in Table 3.2). Fitted semivariogram model parameters were used to perform ordinary kriging (OK) following the same procedures outlined in Section 3.3.2.

Table 3.2. Semivariogram parameters for the sediment composition models.

DATA	n	TYPE OF VARIO-GRAM MODEL	NO. OF LAGS	LAG SIZE (km)[a]	NUGGET	MAJOR RANGE (km)[a]	MINOR RANGE (km)[a]	DIREC-TION (°)[b]	PARTIAL SILL	% OF THE SILL DUE TO THE NUGGET
Mud Fraction	30,126	Exp	50	1.11	0.064	24.44	12.22	82.44	0.15	29.91
Sand Fraction	30,127	Exp	50	1.11	0.082	24.44	12.22	77.87	0.16	33.88
Gravel Fraction	30,115	Exp	50	1.11	0.04	24.44	12.22	141.5	0.045	47.06

a - converted from decimal degrees to kilometers using 111.1 km/decimal degree; b - clockwise from North; Exp = Exponential

Maps representing the predicted fraction for each sediment type were calculated as the sum of the trend (LPI) and residual (kriging) prediction surfaces. The corresponding prediction standard error surfaces were calculated as the square root of the sum of the trend and kriging prediction standard error surfaces (errors in the trend and residual surfaces are assumed to be independent). The final prediction and prediction standard error surfaces were exported as ESRI grids with the extent and spatial resolution described in Section 3.3.1. An error mask was applied to the output grids as described in Section 3.3.2.

Following Goovaerts (1997) and Deutsch and Journel (1998) each sediment type prediction surface was corrected for order violations by setting values less than zero to zero and values greater than one to one and by dividing each prediction value by the sum of the three prediction surfaces where their sum exceeded one. Where the sum was less than one we did not divide by the sum of the prediction surfaces, as some sediment could have been neither mud, sand, nor gravel (e.g., clay).

In addition to the prediction and prediction standard error maps for each sediment type, a vector dataset with polygons classified by sediment texture classes was generated by assigning each grid cell a sediment texture class using the Folk classification scheme (Folk 1954, 1974) based on the predicted ratios of sediment types.

3.3.4. Hard Bottom Occurrence

Data Preparation

An integrated point dataset of known hard bottom locations was built from three sources of seabed survey data and used to develop a prediction surface for the likelihood of hard bottom occurrence. First, we identified locations in the usSEABED Atlantic Coast Offshore Surficial Sediment Data Release, version 1.0 (Reid et al., 2005) parsed and extracted databases where the Shepard code for the point was “solid” or the rock membership value was greater than zero (for description of the rock membership value see Reid et al., 2005). Second, we searched the “National Oceanic and Atmospheric Administration (NOAA)/National Ocean Service (NOS) and U.S. Coast and Geodetic Survey (USCGS) Bottom Type Descriptions from Hydrographic Surveys” database archived at the NOAA National Geophysical Data Center (NOAA NGDC 2011) for point locations where hydrographic survey annotations had described the bottom type as hard or rocky. Third, The Nature Conservancy (TNC) provided a hard bottom point dataset compiled from information in the usSEABED database (Reid et al., 2005) and the National Marine Fisheries Service (NMFS) bottom trawl dataset as part of the Northwest Atlantic Marine Ecoregional Assessment (Greene et al., 2010; J. Greene, The Nature

Conservancy, personal communication, March, 2011; M. Fogarty, NMFS, personal communication, March, 2011). We merged points from these three data sources and removed surveys with identical geographic coordinates. Sample distribution bias can have strong effects on presence-only models (Phillips et al., 2009; Elith et al., 2011). To create a dataset with more uniformly distributed sample effort, we removed hard bottom points in densely surveyed nearshore areas.

Development of the Hard Bottom Occurrence Model

In contrast to other predictive models developed in this report, a geostatistical model could not be applied to the hard bottom point data, because the available hard bottom datasets were restricted to presences, rather than absences, of hard bottom. The lack of absence data arises because hard bottom is very patchily distributed even at very small scales (centimeters to meters). A point sample such as a sediment core that brings up soft sediment does not preclude the presence of hard bottom in the immediate vicinity. Any geostatistical model developed using the unreliable absence data would be heavily biased and uninformative. Reliable absence data for hard bottom generally requires diver, remotely operated vehicle (ROV), photo, video, or acoustic backscatter data that continuously covers large swaths of area; generally impractical in deeper waters.

For this reason, a maximum entropy (MaxEnt) model was used to predict the likelihood of hard bottom occurrence by combining the presence-only hard bottom point dataset with potential predictor variables (Phillips et al., 2006; Phillips and Dudik, 2008). This approach can be thought of as creating a “suitability map” for the presence of hard bottom patches, analogous to habitat suitability maps developed for organisms (Elith et al., 2011). A full description of the MaxEnt algorithm is beyond the scope of this document (see Elith et al., 2011). Briefly, MaxEnt produces an estimate of the relative likelihood of a feature’s occurrence at each location in a specified grid, assuming that presences take on the most spatially random (uniform) distribution possible under the constraint that for each environmental predictor variable the expected value from the estimated distribution matches its observed mean (Elith et al., 2006; Phillips et al., 2006; Peterson et al., 2007). MaxEnt models are trained on a subset of the data and validated by testing predictions on remaining data. MaxEnt has been shown to perform well compared to other presence-only approaches (Elith et al., 2006; Phillips and Dudik, 2008), and is readily implemented using free, open-source software (Phillips et al., 2006, downloadable at http://www.cs.princeton.edu/~schapire/maxent/).

Environmental predictor variables used to train the model of hard bottom occurrence included mean grain size, depth, slope, slope of slope, bathymetric variance, distance from shore, signed distance from shelf, sea surface chlorophyll concentration, and turbidity. All of these predictors are described in Chapters 4 and 6, with the exception of bathymetric variance (calculated as the standard deviation of the depth in ~900 m rectangular neighborhoods). The same transformations described in Appendix 6.B were applied to mean grain size, depth, slope, slope of slope, distance from shore, signed distance from shelf, chlorophyll, and turbidity. Although transformation is not strictly necessary for MaxEnt, we found that transforming predictors improved cross-validation model performance. Eighty percent of the hard bottom presence points were used to build (train) the model and 20% of the points were randomly withheld to test the model. MaxEnt is more robust than regression techniques to the inclusion of large sets of potential predictor variables (Elith et al., 2011), so no model selection was carried out to reduce the size of this predictor set.

MaxEnt provides three post-hoc assessments of the relative importance of predictor variables. First, the MaxEnt program provides a summary of how much each predictor contributes to the gain of the model, accumulated for each predictor over the course of the training algorithm. Second, the MaxEnt program randomly permutes the values for each predictor (one at a time) and determines the resulting decrease in the area under the training model receiver operating characteristic curve (AUC). This provides a measure of how strongly the model depends on each predictor. Third, the MaxEnt program estimates predictor importance using a jackknife approach, in which it re-runs the model for each predictor, first building the model with all variables except the predictor of interest, and then building the model with only the predictor of interest. If a predictor is highly correlated with the other predictors, withholding it will have little impact on model performance. Therefore, an important and non-redundant predictor will have high explanatory power by itself and its omission from the model will result in a significant reduction in predictive power.

The final map of the "hard bottom occurrence likelihood index" consisted of a logistic transformation of MaxEnt's raw output to produce a smooth index between 0 and 1 (this is the default output of the MaxEnt program). It is related to the probability of occurrence, but is not strictly a probability (Elith et al., 2011). It should be considered an index of the relative likelihood of hard bottom occurrence, rather than a strict measure of the probability of encountering hard bottom. All of the issues and caveats related to interpretation of ecological models based on presence-only data are applicable (Elith et al., 2011).

3.3.5. Model Validation

The performance of mean grain size and sediment composition models was evaluated by two methods: leave-one-out cross-validation and qualitative comparison to an independent sidescan sonar backscatter dataset. Leave-one-out cross validation of kriging predictions was performed in ESRI Geostatistical Analyst (ESRI 2011a) as described in Goovaerts (1997). Cross-validation statistics were calculated as described in ESRI (2011b).Qualitative comparisons to acoustic backscatter data followed Goff et al. (2008). Model prediction maps were presented alongside existing 100-120 kHz backscatter data collected by USGS in the New York Bight region (Schwab et al., 2000; Schwab et al., 2002) and visually interpreted. In general, acoustic backscatter intensity is lower where there are fine sediments and higher where there are coarse sediments (Ferrini and Flood, 2006; DeFalco et al., 2010).

In addition to qualitative comparison with acoustic backscatter data, the hard bottom occurrence model performance was evaluated using cross-validation on the 20% of data withheld from training. Cross-validation performance was evaluated using the Area-Under-Curve (AUC) statistic of the receiver operating characteristic (ROC)-like MaxEnt output (Fielding and Bell, 1997). Traditional ROC curves plot the true positive rate (sensitivity) versus the false positive rate (1 – specificity) for the range of potential threshold values, with the AUC statistic providing a measure of how well the model maximizes the true positive rate for low values of the false positive rate. The AUC statistic ranges from 0.5 (no better than random) to 1.0 (a perfect prediction). An AUC statistic greater than 0.75 is generally indicative of a potentially useful model, and ROC curves for high performing models will approach the upper left corner of the plot (Fielding and Bell, 1997; Peterson et al., 2007). The ROC-like analysis used by MaxEnt differs in that it substitutes the fractional predicted area for the specificity since there is no absence data from which to measure specificity (the true negative rate). As a result the maximum achievable AUC is less than one (Phillips et al., 2006).

3.4. RESULTS AND DISCUSSION

3.4.1. Mean Grain Size

Model Predictions

The model of mean grain size extended just past the continental shelf edge and provided predictions of mean grain size for the majority of the study area. The model did not extend into Long Island Sound (LIS) because Goff et al. (2008) did not include LIS in their quality-controlled dataset. An additional reason for excluding LIS was that the geostatistical model developed for the open ocean system (most of the study area) would not have applied to the geomorphologically distinct, enclosed Long Island Sound system. The model did not extend far past the continental shelf edge due to lack of sufficient sampling effort. The model predicted that much of the seafloor is covered by sediment with a mean grain size characteristic of coarse to medium sand (0-2 φ), with areas having mean grain size characteristic of finer sand and silt (4-6 φ) within the upper reaches of the Hudson Shelf Valley, offshore of the shelf break, and in the area of the Block Island Delta and Block Island Valley. The model predicted that mean grain sizes characteristic of coarse to medium sand covered ~60% of the study area, mean grain sizes characteristic of fine to very fine sand covered ~32% of the study area and mean grain sizes characteristics of silt covered ~8% of the study area (Figure 3.1, Figure 3.2, Table 3.3).

Model Uncertainty

Model standard error ranged from ~1.2 φ units for grid cells with a very high density of seafloor surveys to ~1.6 φ units for grid cells farthest from survey locations, such as the area farthest offshore (Figure 3.3). Model uncertainty of this magnitude corresponds to theoretical 95% confidence intervals (±1.96*standard error) ranging from the mean grain size prediction ± 2.4 φ units in densely surveyed areas to the prediction ± 3.2 φ units where surveys were more sparse. For example, a mean grain size prediction of 1 φ in a densely

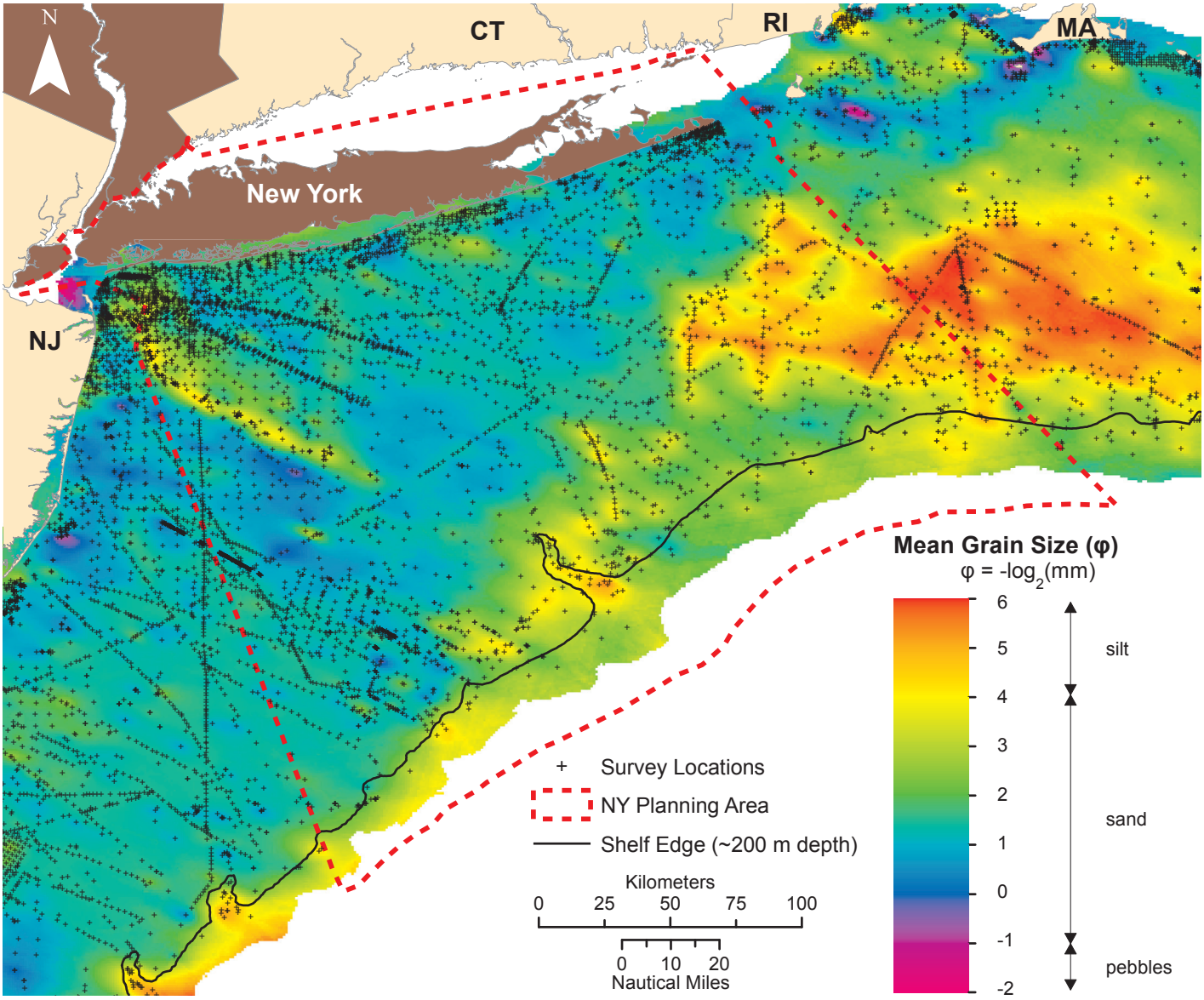

Figure 3.1. Predicted mean grain size of surficial sediments from kriging interpolation of mean grain size data in the Mid-Atlantic Bight. Mean grain size is in φ units, where φ = -log$_2$(mean grain diameter in mm). Data courtesy of J. Goff (University of Texas at Austin), derived from USGS usSEABED database (Reid et al., 2005).

surveyed area could have a theoretical 95% confidence interval of (-1.4 φ, 3.4 φ). In this case, the mean grain size prediction corresponds to coarse sand, but the confidence interval limits range from very fine pebbles to very fine sand. Given that sediment surveys in areas offshore of the continental shelf break were quite sparse and prediction accuracy in these areas is worse than in nearshore areas, model predictions offshore of the shelf break should be used with caution.

The predicted probabilities of exceeding mean grain size thresholds of 25.6 cm (φ < -8, boulders and larger), 6.4 cm (φ < -6, cobbles and larger), 2 mm (φ < -1, pebbles and larger), and 0.062 mm (φ < 4, very fine sand and larger) generally followed spatial patterns in mean grain size predictions. This is expected since these probability calculations assume a normal distribution of sediment grain sizes around the mean. The probabilities of having a mean grain size less than -8 φ (boulders and larger) or less than -6 φ (cobbles and larger) were essentially zero across the entire study area (Figure 3.4a, b). This does not mean that boulders and cobbles do not occur, only that they are almost never the mean grain size over any appreciable area (they are always mixed with other, finer sediment types), and/or they are very erratic in their occurrence (occurring only as isolated departures from the mean). The probability of having a mean grain size less than -1 φ (pebbles and larger) was very low across most of the study area, but there were areas of higher probability corresponding

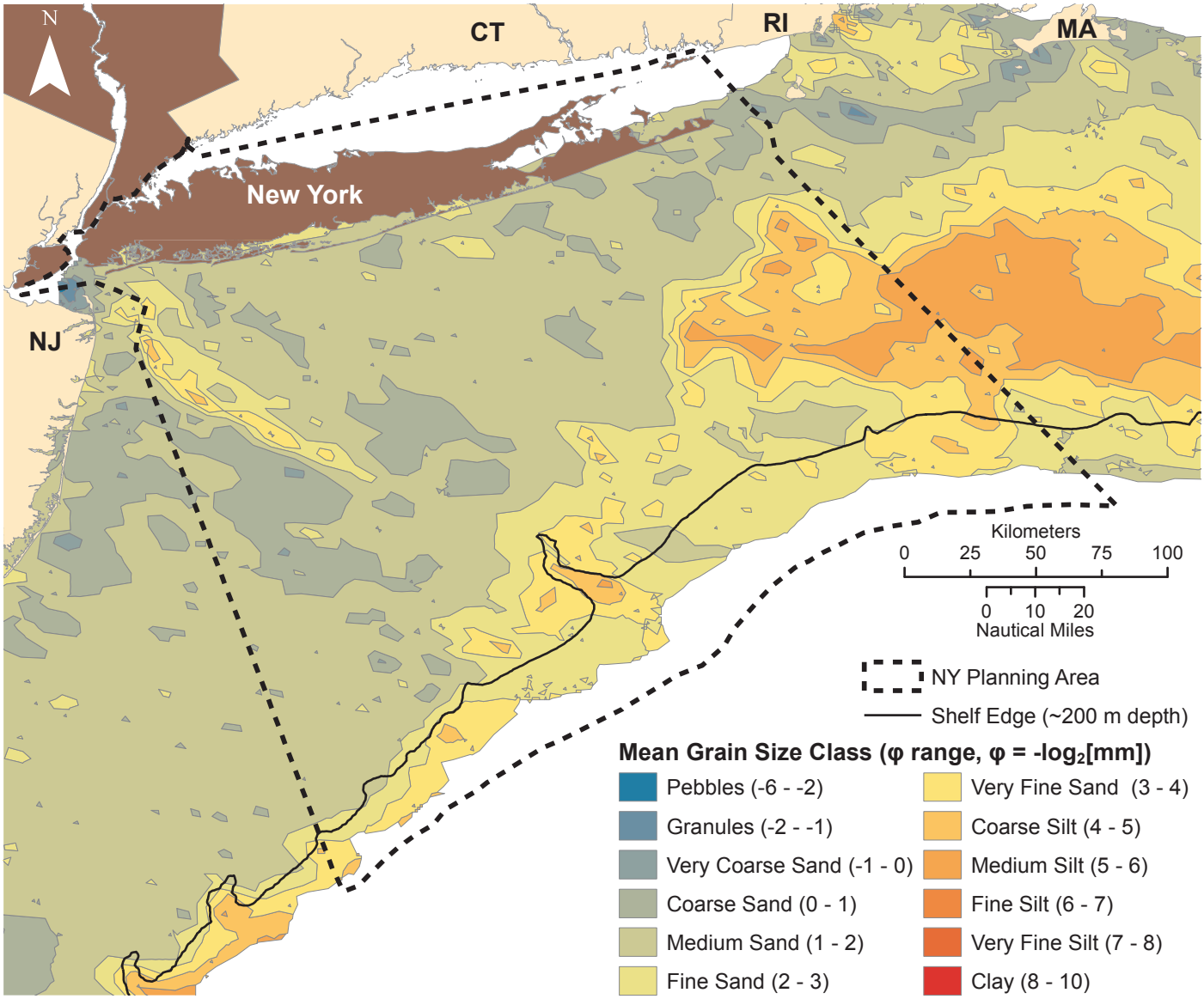

Figure 3.2. Distribution of predicted surficial sediment mean grain size classes, derived from kriging interpolation of mean grain size data in the Mid-Atlantic Bight. Mean grain size classes are defined based on Wentworth (1922). Data courtesy of J. Goff (University of Texas at Austin), derived from USGS usSEABED database (Reid et al., 2005).

Table 3.3. Total area and percent area of predicted mean grain size classes in the study area.

MEAN GRAIN SIZE CLASS[a]	MEAN GRAIN SIZE (Φ)[b]	MEAN GRAIN SIZE (METRIC)	PREDICTED TOTAL AREA (km^2)	PREDICTED PERCENT AREA
Pebbles	-6 – -2	4 mm – 6.4 cm	1	0
Granules	-2 – -1	2 mm – 4 mm	12	0
Very Coarse Sand	-1 – 0	1 mm – 2 mm	38	0.1
Coarse Sand	0 – 1	0.5 mm – 1 mm	4,978	12.2
Medium Sand	1 – 2	0.25 mm – 0.5 mm	19,613	47.9
Fine Sand	2 – 3	0.125 mm – 0.25 mm	8,607	21.0
Very Fine Sand	3 – 4	0.062 mm – 0.125 mm	4,402	10.8
Coarse Silt	4 – 5	0.031 mm – 0.062 mm	2,525	6.2
Medium Silt	5 – 6	0.016 mm – 0.031 mm	734	1.8
Fine Silt	6 – 7	0.008 mm – 0.016 mm	0	0
Very Fine Silt	7 – 8	0.004 mm – 0.008 mm	0	0
Clay	8 – 10	0.001 mm – 0.004 mm	0	0

a - from Wentworth (1922)

b - $\varphi = -\log_2$(mean grain diameter in mm)

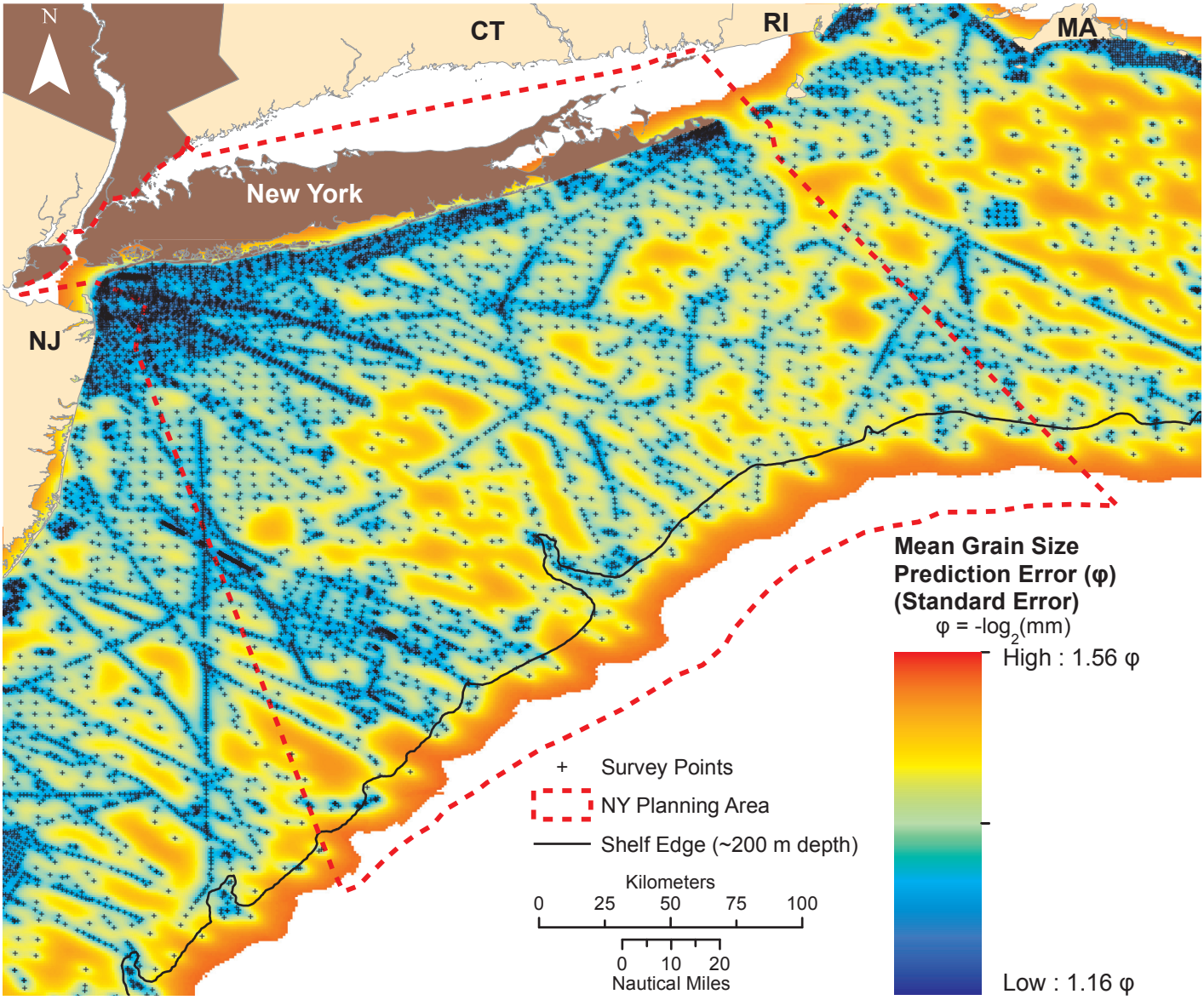

Figure 3.3. Surficial sediment mean grain size prediction standard error (in φ units, φ = -log$_2$[mean grain diameter in mm]) from kriging interpolation of the mean grain size data in the Mid-Atlantic Bight. Data courtesy of J. Goff (University of Texas at Austin), derived from USGS usSEABED database (Reid et al., 2005).

well with the areas mapped as pebbles by the mean grain size prediction model (Figure 3.1, Figure 3.4c). The probability of having a mean grain size less than 4 φ (very fine sand and larger) was high across the study area, with areas of near zero probability corresponding to areas that were mapped as silt (Figure 3.1, Figure 3.4d).

Probabilities for each mean grain size threshold were also mapped with values standardized by the maximum probability values (Figure 3.5). These maps emphasize areas where the mean grain size has the highest relative likelihood of exceeding the indicated thresholds. Panels (a) and (b) of Figure 3.5 should be interpreted with some caution since the highest probabilities are near zero for thresholds of less than -8 φ (boulders and larger) or less than -6 φ (cobbles and larger).

Model Validation

Leave-one-out cross-validation of the mean grain size prediction model yielded a root-mean-square error (RMSE) of 1.4 φ, which was reasonable given the magnitude of grain size measurement error (estimated to be on the order of 1 φ unit; J. Goff, University of Texas at Austin, personal communication, February 11,

2011) and allowing for unresolved small-scale variance and model specification error. Cross-validation also indicated that the prediction errors were unbiased (mean standardized prediction error was near zero) and the assessment of prediction uncertainty was valid since the root-mean-square standardized error was close to one (Table 3.4).

Although the mean grain size prediction model was mapped at a considerably lower spatial resolution (30 arc-second grid cells have an average linear dimension of ~800-900 meters in the study area) than the USGS acoustic backscatter data (4 m grid cells) from Schwab et al. (2002), comparison of the mean grain size prediction map to the USGS backscatter data provided a qualitative assessment of the accuracy of the predictions for overlapping areas. In general, areas of high backscatter intensity (lighter shades) were associated with areas predicted to have coarser sediments, such as the areas labeled A and C in Figure 3.6. Also, the Hudson Shelf Valley (area labeled B in Figure 3.6) had low backscatter intensity and was predicted to have finer sediments. These comparisons were consistent with the conclusions of Ferrini and Flood (2006) and De Falco et al. (2010), who found that acoustic backscatter intensity is generally lower where there are fine sediments and higher where there are coarse sediments. However, the matchup is clearly not perfect, and without detailed calibration of backscatter to ground-truth samples it is difficult to say whether deviations between the two maps are due to inaccurate model predictions or variation in the backscatter surface not associated with sediment variation.

3.4.2. Sediment Composition

Model Predictions

Models of sediment composition provided predictions for most of the study area, from the southern shore of Long Island, where survey density was greatest, to just past the continental shelf edge (Figure 3.7).

The mud fraction model predicted that seafloor surficial sediments were composed

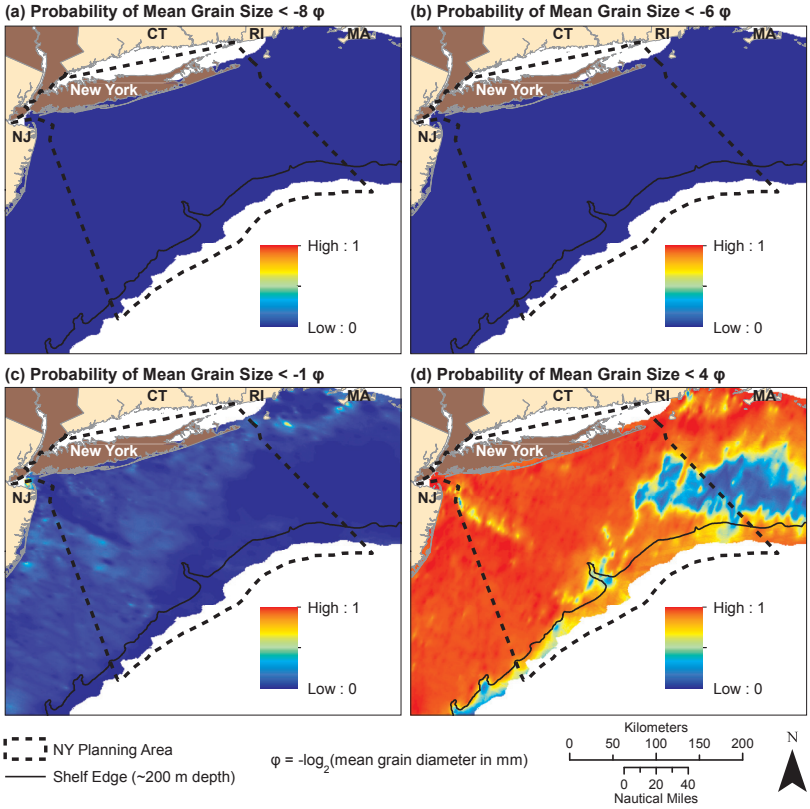

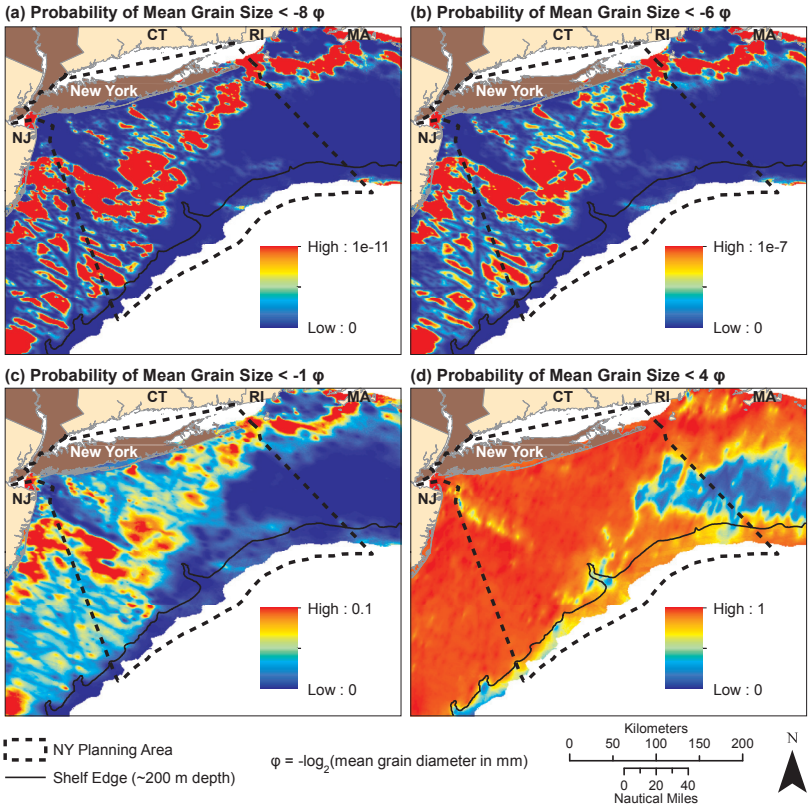

Figure 3.4 (top). Maps of the probability that surficial sediment mean grain size (in φ units, φ = -log$_2$[mean grain diameter in mm]) is less than threshold values of (a) -8 φ (boulders and larger), (b) -6 φ (cobbles and larger), (c) -1 φ (pebbles and larger), and (d) 4 φ (sand and larger). Figure 3.5 (bottom). Same as Figure 3.4, with probability values standardized by maximum probability of each corresponding threshold map. Values were adjusted to emphasize areas with the highest probabilities of exceeding each of the mean grain size thresholds. Data courtesy of J. Goff (University of Texas at Austin), derived from USGS usSEABED database (Reid et al., 2005).

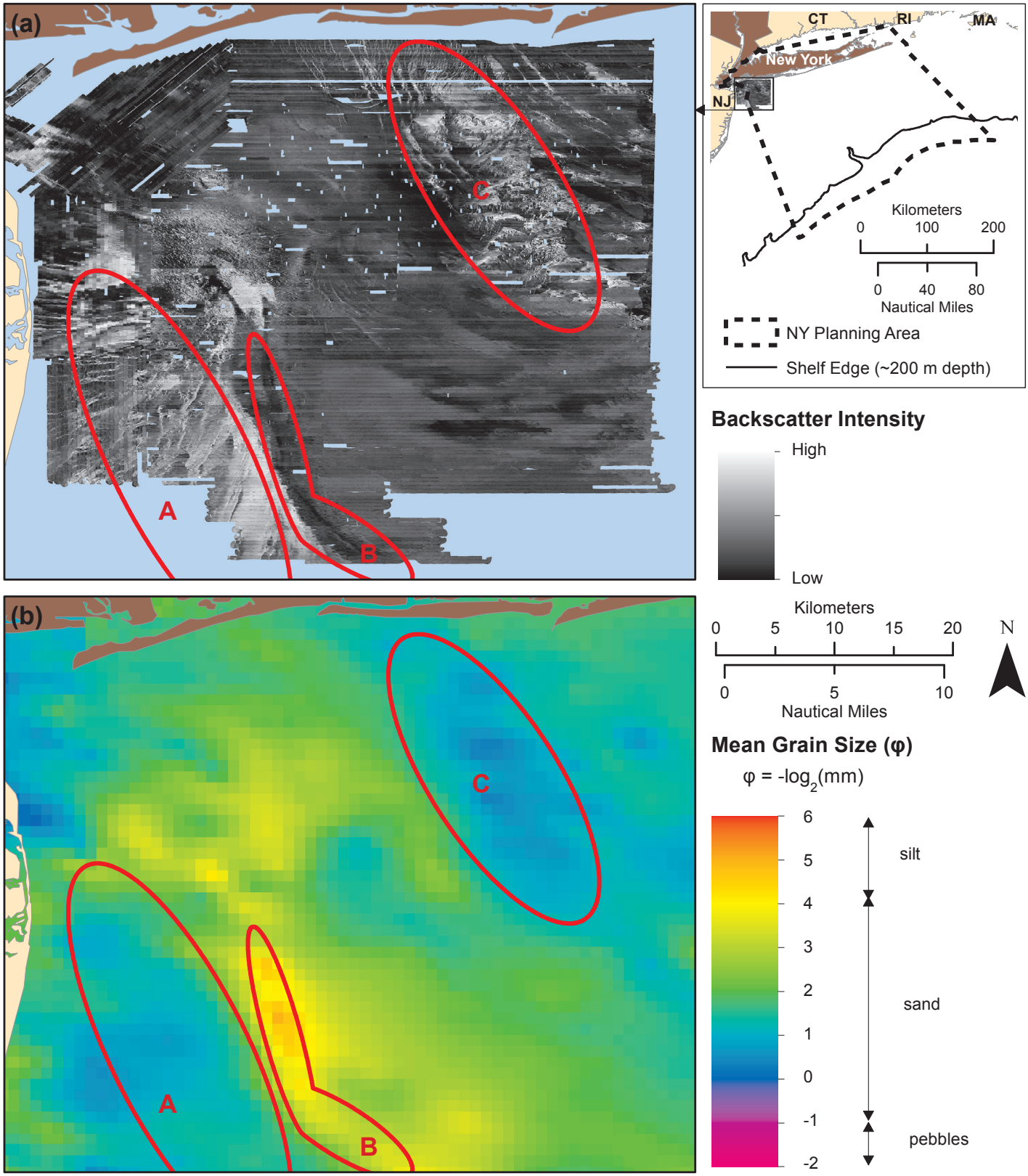

Figure 3.6. Comparison of overlapping portions of the (a) USGS acoustic backscatter data (from Schwab et al., 2002) and (b) surficial sediment mean grain size prediction (in φ units, $\varphi = -\log_2$[mean grain diameter in mm]). In general, higher backscatter intensity indicates coarser sediments (e.g., coarse sand, pebbles) while lower backscatter intensity indicates finer sediments (e.g., sand and silt). Mean grain size data courtesy of J. Goff (University of Texas at Austin), derived from USGS usSEABED database (Reid et al., 2005).

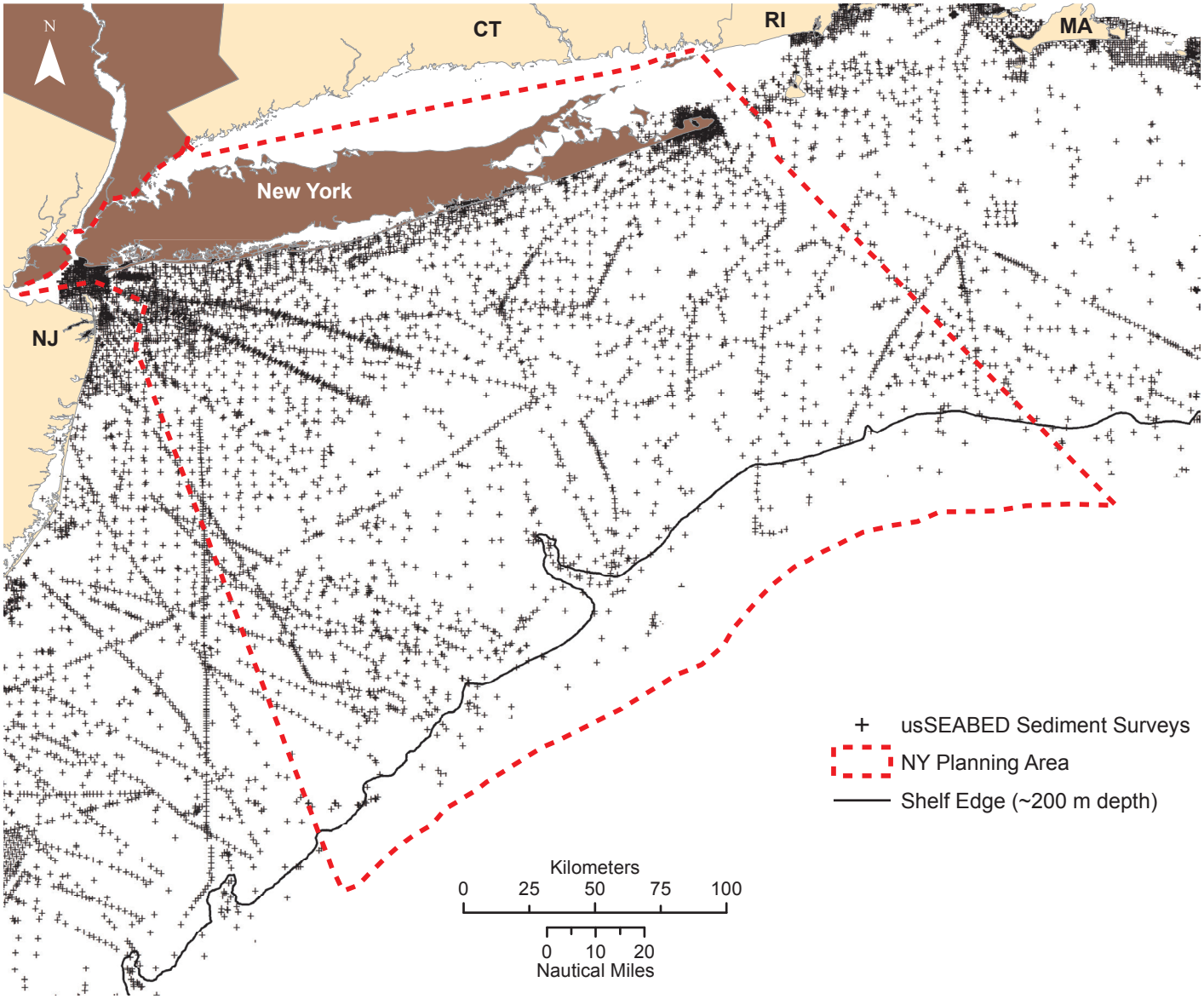

Figure 3.7. Locations of usSEABED sediment survey data in the study area. Data courtesy of USGS usSEABED database (Reid et al., 2005).

mostly of mud in several areas, including in the Hudson Shelf Valley, in and around the Hudson Canyon, along the continental shelf slope, and over a large swath south of Martha's Vineyard and Rhode Island between the 50 m and 100 m contours (Figure 3.8a). The sand fraction model predicted that surficial sediments were composed mostly of sand throughout most of the study area (Figure 3.8b), with the exception being those areas predicted to have mud-dominated sediments by the mud fraction model. The gravel fraction model predicted that surficial sediments were composed mostly of gravel in only a few small areas (Figure 3.8c). These areas corresponded to those mapped as pebbles or granules by the model of mean grain size (Figure 3.1). Under Folk's classification scheme (Folk 1954, 1974), just over half of the study area was mapped as gravelly sand or slightly gravelly sand (Figure 3.8d, Table 3.5). Another ~30% of the study area was mapped as having a mix of mud and sand with slight amounts of gravel. An almost negligible area was mapped as having predominantly gravel.

Table 3.4. Cross-validation statistics for the mean grain size model.

DIAGNOSTIC STATISTIC	VALUE
Bias	-0.0007
Root-Mean-Square Error (RMSE)	1.4090
Mean Standardized Prediction Error	-0.0004
Root-Mean-Square Standardized Error	1.0920

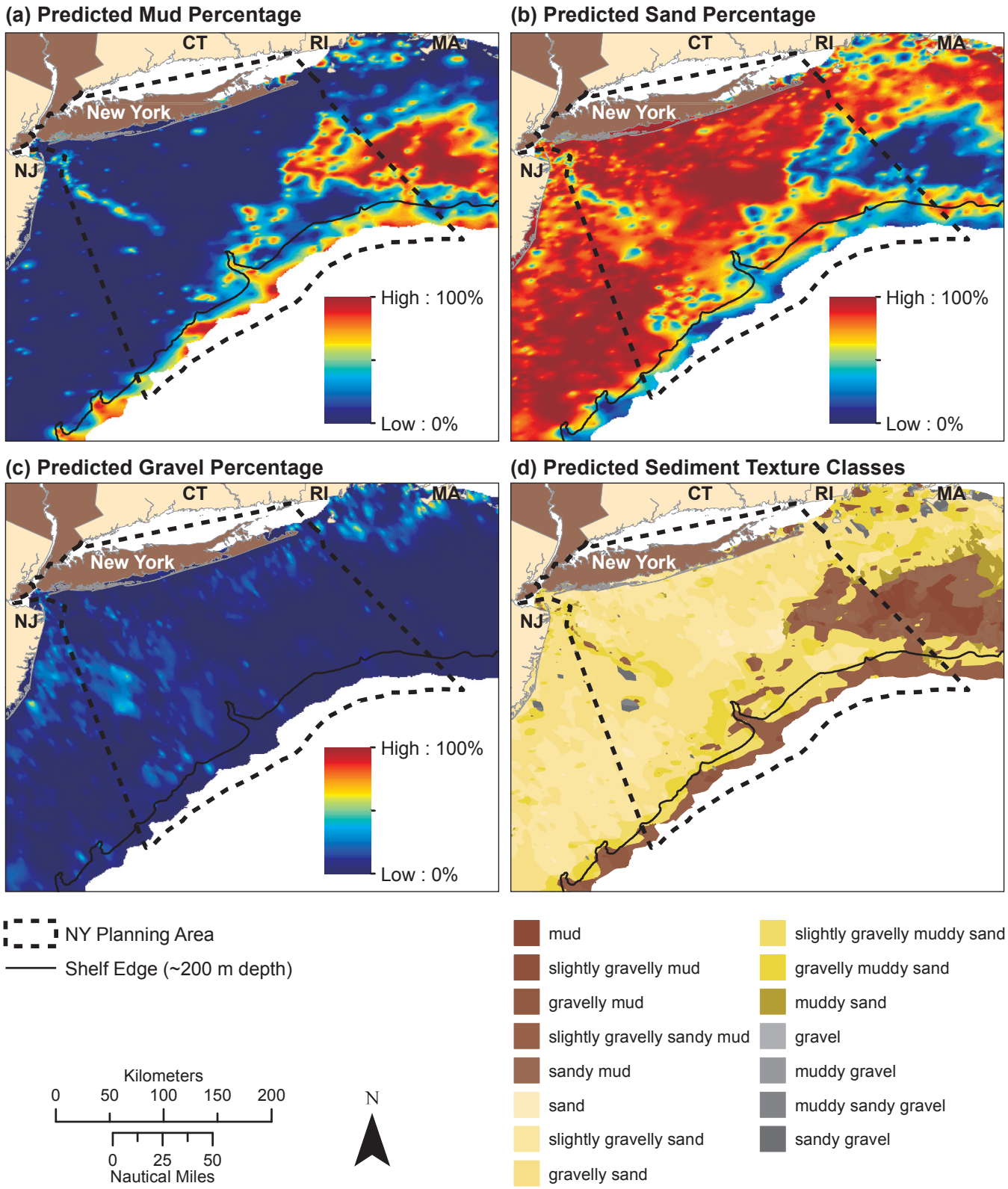

Figure 3.8. Surficial sediment composition maps from kriging interpolations of usSEABED sediment composition data in the Mid-Atlantic Bight. (a) Predicted mud percentage, (b) predicted sand percentage, (c) predicted gravel percentage, (d) distribution of predicted sediment texture classes. Sediment texture classes were assigned based on the ratios of the predicted mud, sand, and gravel fractions according to Folk (1954, 1974). Data courtesy of USGS usSEABED database (Reid et al., 2005).

Model Uncertainties

For all three sediment types, model uncertainties were lowest in densely surveyed areas and highest in unsurveyed areas, particularly farthest offshore of the continental shelf break. Model prediction standard error was lowest for the gravel fraction model (Figure 3.9), which was the least encountered sediment type in sediment samples. As with the mean grain size model, given that sediment surveys in areas offshore of the continental shelf break were sparse and prediction accuracy in these areas is worse than in nearshore areas, model predictions offshore of the shelf break should be used with caution.

Model Validation

Cross-validation of the sediment composition models yielded RMSE values ranging from 23% for gravel to 32% for sand (Table 3.6). The somewhat high RMSE values were not surprising given the heterogeneous nature of the data (laboratory analyzed vs. interpretation of written descriptors) and the potential bias toward finer particles for some of the sediment surveys (discussed in Goff et al., 2008). Cross-validation indicated that prediction errors were unbiased (mean standardized prediction errors were near zero) and the assessments of prediction uncertainty were valid since the root-mean-square standardized errors were close to one (Table 3.6). Given the relatively high RMSE values, all three sediment composition models should be used with caution and with the knowledge that available data can only provide moderately reliable predictions at investigated spatial scales. Although there are discernible broad-scale spatial patterns, the composition of sediment in any given point sample is highly variable and difficult to predict.

The gravel fraction prediction model was compared to USGS acoustic backscatter data from Schwab et al. (2002) to provide a qualitative accuracy assessment of predictions for overlapping areas. Although the gravel fraction model was mapped at a considerably coarser spatial resolution (~800-900 m grid cells) than the backscatter data (4 m grid

Table 3.5. Total area and percent area of predicted sediment texture classes in the study area.

SEDIMENT TEXTURE CLASS[a]	DESCRIPTION[a]	PREDICTED TOTAL AREA (km^2)	PREDICTED PERCENT AREA
mud	"gravel < 0.01%, sand : mud < 1:9"	61	0.1
slightly gravelly mud	"0.01-5% gravel, sand : mud < 1:9"	408	1.0
gravelly mud	"5-30% gravel, sand : mud < 1:1"	788	1.9
slightly gravelly sandy mud	"0.01-5% gravel, sand : mud from 1:9 to 1:1"	5158	12.6
sandy mud	"gravel < 0.01%, sand : mud from 1:9 to 1:1"	918	2.2
sand	"gravel < 0.01%, sand : mud > 9:1"	774	1.9
slightly gravelly sand	"0.01-5% gravel, sand : mud > 9:1"	9,352	22.9
gravelly sand	"5-30% gravel, sand : mud > 9:1"	12,353	30.2
slightly gravelly muddy sand	"0.01-5% gravel, sand : mud from 1:1 to 9:1"	6,812	16.7
gravelly muddy sand	"5-30% gravel, sand : mud from 1:1 to 9:1"	3,488	8.5
muddy sand	"gravel < 0.01%, sand : mud from 1:1 to 9:1"	472	1.2
gravel	> 80% gravel	0	0
muddy gravel	"30-80% gravel, sand : mud < 1:1"	11	0
muddy sandy gravel	"30-80% gravel, sand : mud from 1:1 to 9:1"	87	0.2
sandy gravel	"30-80% gravel, sand : mud > 9:1"	211	0.5

a - from Folk 1954, 1974.

Table 3.6. Cross-validation statistics for the sediment composition models.

	SEDIMENT COMPOSITION MODEL		
Diagnostic Statistic	**Mud Fraction**	**Sand Fraction**	**Gravel Fraction**
Bias	-0.000004	-0.000420	0.000140
Root-Mean-Square Error (RMSE)	0.266200	0.320800	0.227200
Mean Standardized Prediction Error	-0.000076	-0.000620	0.000340
Root-Mean-Square Standardized Error	0.862400	0.943400	1.005900

cells), a general spatial correspondence was observed over broad spatial scales. Areas of high backscatter intensity (lighter shades) were generally associated with areas predicted to be gravelly (A and C in Figure 3.10) and the narrow region of low backscatter intensity in the Hudson Shelf Valley (B in Figure 3.10) roughly corresponded to areas predicted to be sand or mud. As noted previously, the matchup is clearly not perfect, and without detailed calibration of backscatter to ground-truth samples it is difficult to say whether deviations between the two maps are due to inaccurate model predictions or variation in the backscatter surface not associated with sediment variation.

3.4.3. Hard Bottom Occurrence

Model Prediction

The MaxEnt model output indicated a relatively high likelihood of hard bottom occurrence in nearshore areas and in the vicinity of canyon features just offshore of the continental shelf break (e.g., Hudson Canyon) (Figure 3.11). The model also corresponded well to the mean grain size model in that it predicted a low likelihood of hard bottom occurrence in areas mapped as fine particles. It is important to note that the model does not provide any indication of the size of predicted hard bottom features, and does not necessarily relate to the proportion of substrate that is hard bottom at a given location. Rather, the model provides a relative index of the likelihood that at least one hard bottom point would occur if an area was sampled a sufficient number of times. An area predicted as having a high likelihood of hard bottom occurrence may in fact be dominated by non-hard bottom substrate. For example, the nearshore areas in the study area were predicted to have a high likelihood of hard bottom occurrence by the MaxEnt model, but the mean grain size and sand fraction models suggest they are predominantly sandy. Taken together, the models suggest that the nearshore areas have a surface composed primarily of sandy sediments but with widely distributed (although not abundant) hard bottom components such as large boulders, bedrock, or highly consolidated sediments. This example stresses the importance of supplementing information derived from one aspect of sediment character (e.g., mean grain size) with additional information to provide a more complete characterization of surficial sediment distribution.

The MaxEnt model output indicated that the predictor variables distance from shore, slope of slope, depth, and signed distance from shelf were most important in determining the distribution of hard bottom presences, relative to the other predictors included in the set, when measured in terms of their contribution to regularized model gain (Table 3.7). According to the jack-knifing outputs, signed distance from shelf, distance from shore, and depth had the greatest individual predictive power (Figure 3.12). The model built without signed distance to shelf showed a significant decrease in gain, which suggested that this predictor was important and not redundant (i.e., not highly correlated with other predictors). Interestingly, surface

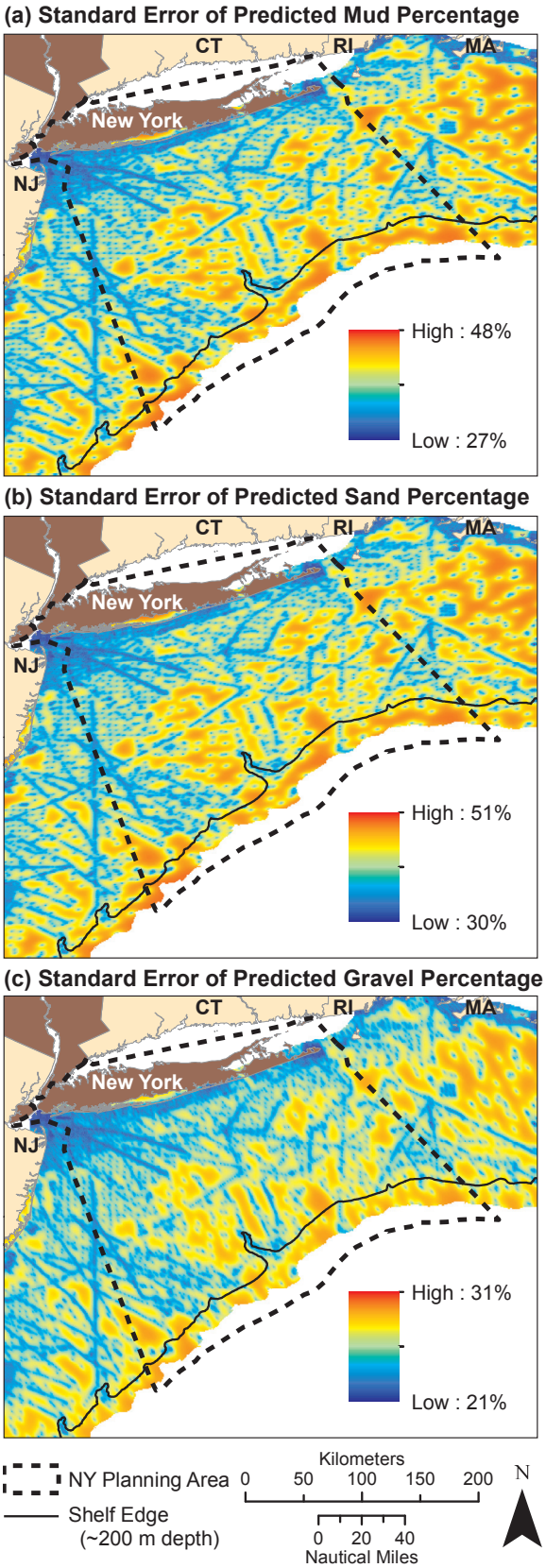

Figure 3.9. Standard error maps for (a) predicted mud percentage, (b) predicted sand percentage, and (c) predicted gravel percentage of surficial sediments from kriging interpolations of usSEABED sediment composition data in the Mid-Atlantic Bight. Data courtesy of USGS usSEABED database (Reid et al., 2005).

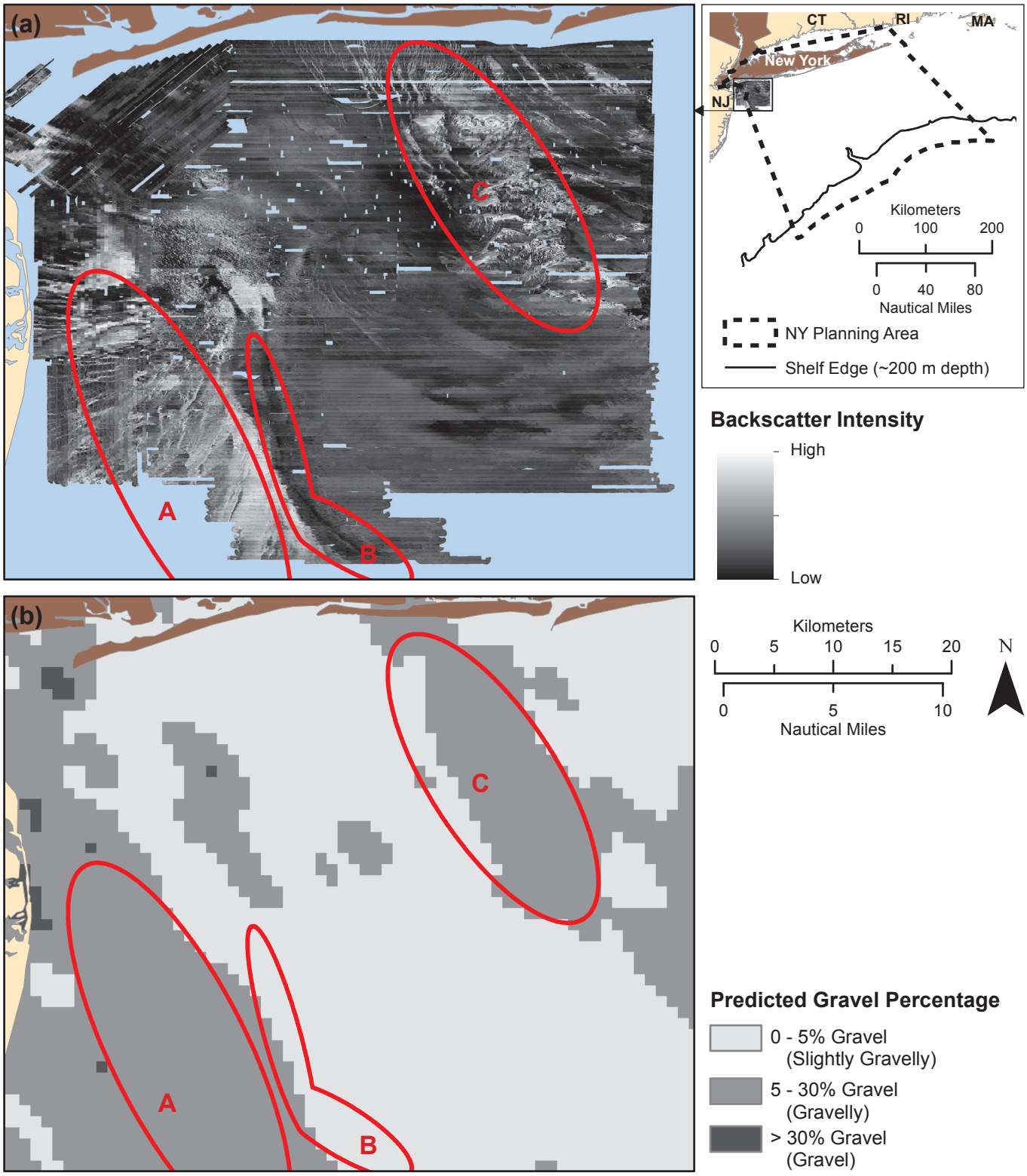

Figure 3.10. Comparison of overlapping portions of the (a) USGS acoustic backscatter data (from Schwab et al., 2002) and (b) the predicted gravel percentage in surficial sediments. In general, higher backscatter intensity indicates coarser sediments (e.g., gravel) while lower backscatter intensity indicates finer sediments (e.g., sand and mud). Sediment survey data courtesy of USGS usSEABED database (Reid et al., 2005).

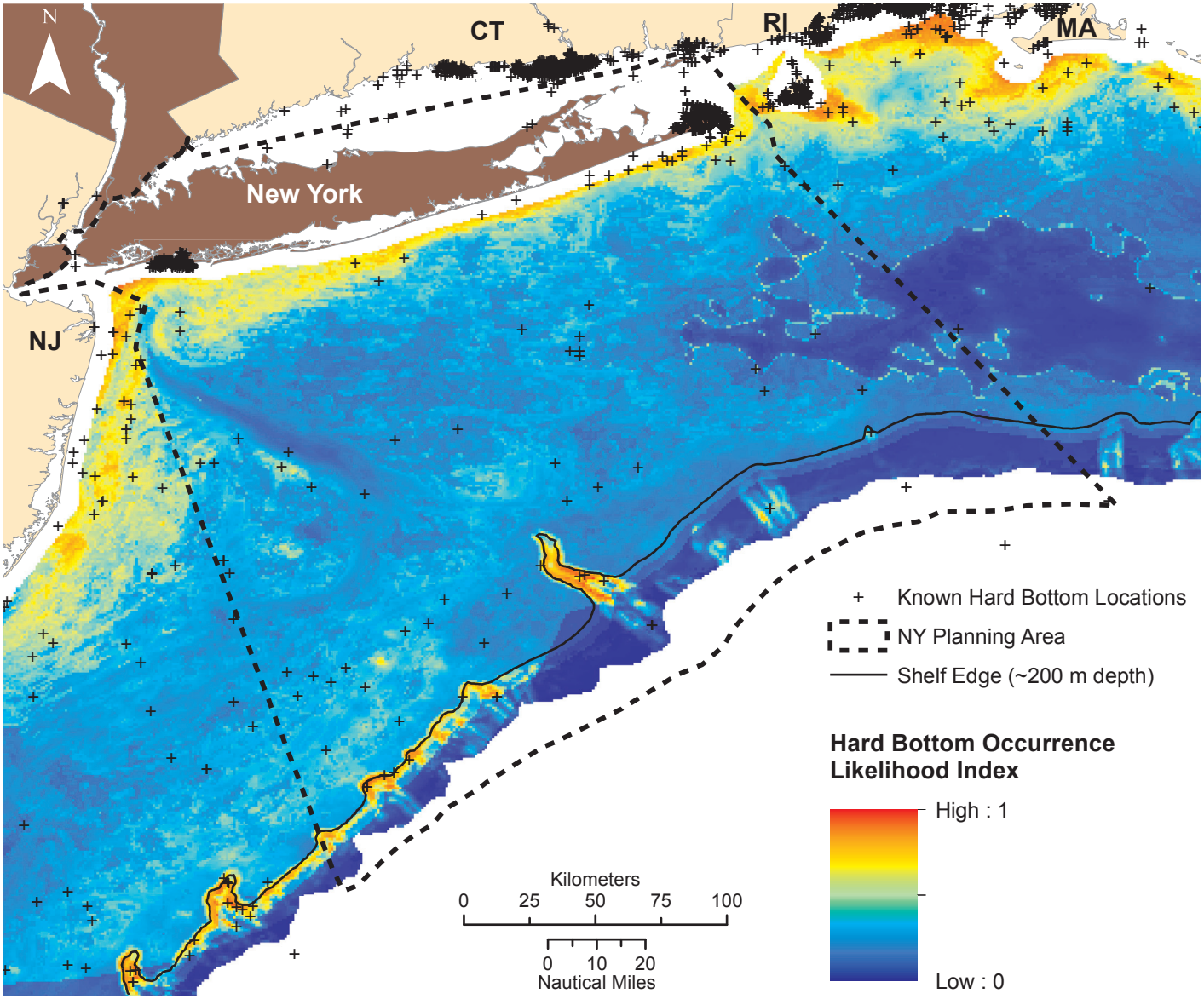

Figure 3.11. MaxEnt model of hard bottom occurrence. Map depicts the predicted relative likelihood of hard bottom occurrence from the maximum entropy model. Data courtesy of USGS usSEABED database (Reid et al., 2005), NOS Hydrographic (NOAA NGDC 2011), and The Nature Conservancy (Greene et al., 2010; J. Greene, The Nature Conservancy, personal communication, March, 2011; M. Fogarty, NMFS, personal communication, March, 2011).

chlorophyll concentration had low predictive power by itself, but its omission resulted in the greatest decrease in the predictive power of the model. This suggested that important information may be contained in the interaction of surface chlorophyll concentration with one or more of the other predictors.

Model Validation

The MaxEnt ROC-like analysis indicated good model performance, with a training AUC of 0.832 and test AUC of 0.730 (Figure 3.13). This indicates that ~73% of the time a randomly selected true hard bottom location will have a higher predicted probability of hard bottom presence than would any randomly selected location in the study area.

Table 3.7: Relative contributions of predictor variables to the MaxEnt model for hard bottom occurrence (based on cumulative regularized gain estimates).

PREDICTOR VARIABLE	PERCENT CONTRIBUTION
distance from shore	26.4
slope of slope	17.6
depth	16.0
signed distance from shelf	15.0
mean grain size	8.9
slope	6.8
surface chlorophyll concentration	4.1
turbidity	3.3
bathymetric variance	1.9

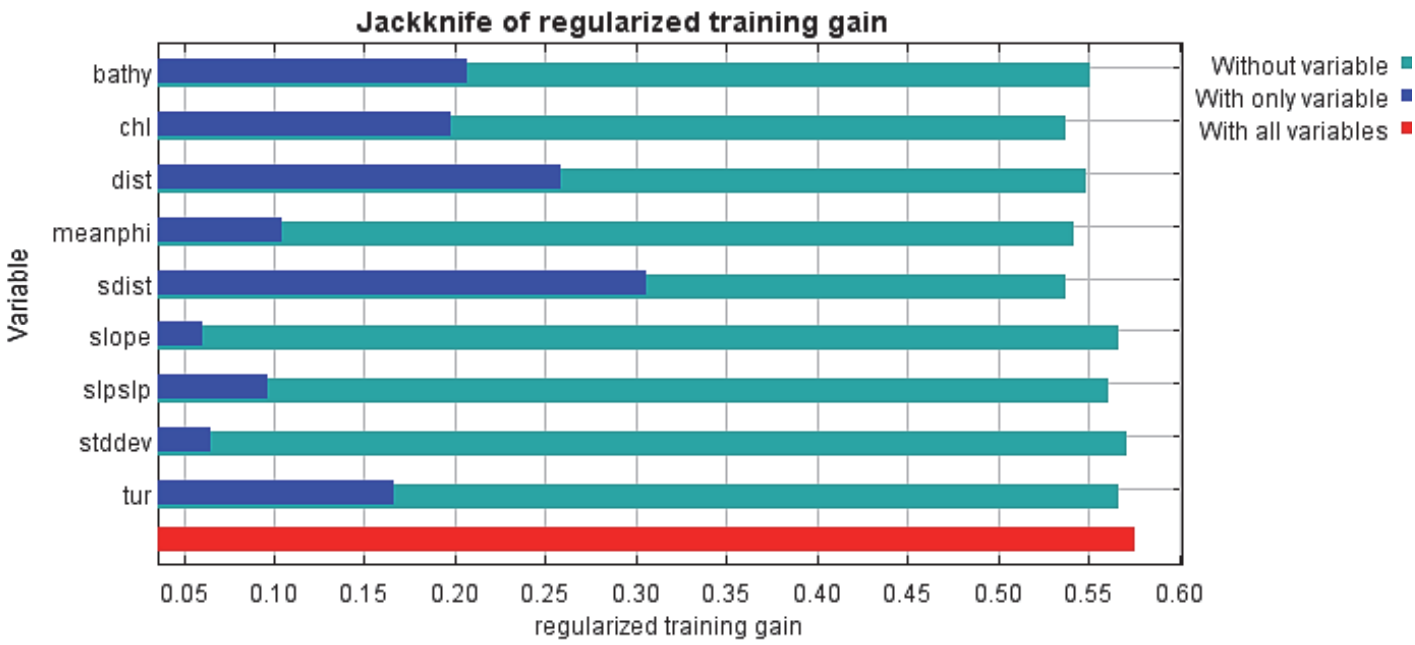

Figure 3.12. Jackknife test of predictor variable importance for the MaxEnt model of hard bottom occurrance. Blue bars indicate regularized training gain for models built with each predictor individually. Green bars indicate regularized training gain for models built with all other predictors and can be compared to the red bar, which indicates the regularized training gain for a model built using all the predictors, to determine how much the regularized training gain decreases with the omission of each predictor. Predictor variables: bathy = depth, chl = sea surface chlorophyll concentration, dist = distance from shore, meanphi = sediment mean grain size, sdist = signed distance from shelf, slope = slope, slpslp = slope of slope, stddev = bathymetric variance, tur = turbidity.

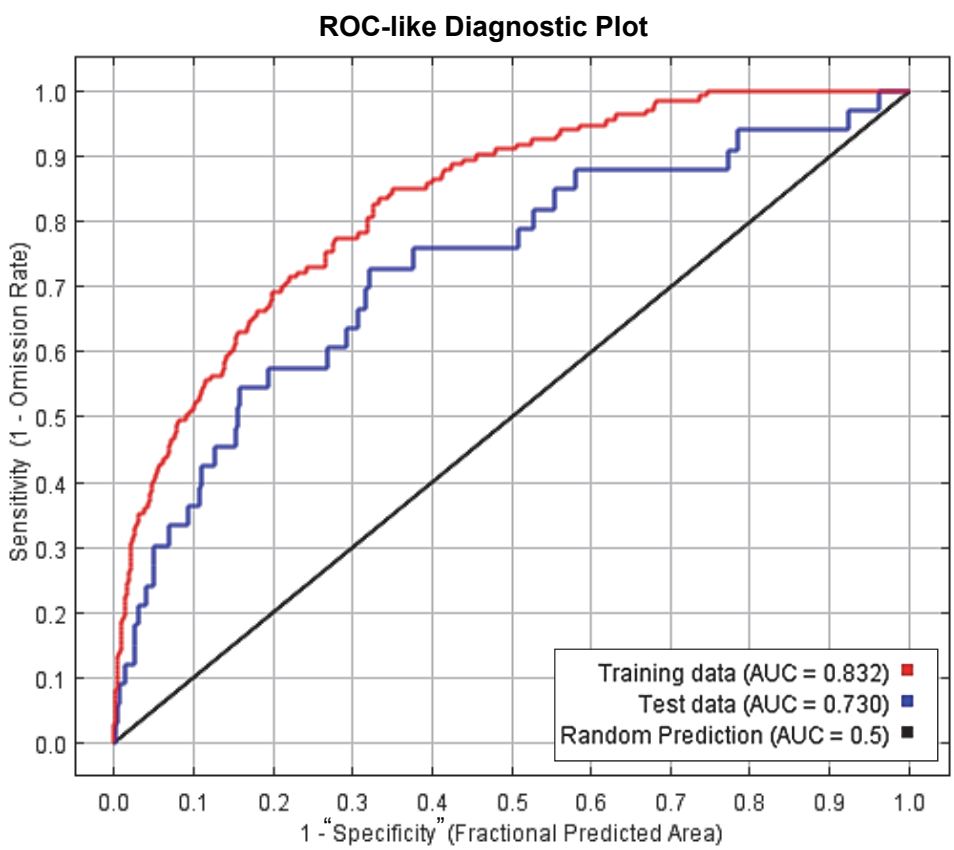

Figure 3.13. Receiver operating characteristic-like (ROC-like) curve for the MaxEnt model of hard bottom occurrence.

Although the model was mapped at a considerably lower spatial resolution (30 arc-second grid cells have an average linear dimension of ~800-900 m in the study area) compared to the USGS acoustic backscatter data (4 m grid cells) from Schwab et al. (2002), comparison of the predicted hard bottom occurrence likelihood index map to the USGS backscatter data revealed some qualitative spatial association between areas of high backscatter intensity (lighter shades) and areas predicted to have a high probability of hard bottom presence by the model (Figure 3.14).

3.5. Limitations to Interpretation

Mean Grain Size and Sediment Composition Models

As with the bathymetry model (Chapter 2), the density of usSEABED survey locations affected mean grain size and sediment composition model uncertainty estimates. In the study area, survey density was highest nearshore and was considerably lower in offshore areas. Although the mean grain size model and sediment composition models seemed to capture meso-scale (10's to 100's of km) spatial patterns across the study area (e.g., predictions of silt in major depositional areas), the models likely missed finer scale patterns in sediment distribution, especially in areas where the spatial density of sampling was low. The length scale of features that can be resolved will generally be no shorter than twice the local average distance between samples. Regardless of sample density, because the spatial resolution of the output model grid is approximately 800 m, the minimum length scale of features that can be resolved is approximately 1.6 km. While sediment survey density in nearshore areas may support the development of a model at a finer spatial resolution, areas with fewer survey data (such as offshore of the continental shelf break) limit the resolving power of the model. As a result, none of the models presented in this chapter can be used to directly predict the locations of smaller features such as hard bottom patches or cold water coral reefs.

There are also limitations to the reliability of the mean grain size and sediment composition models that are related to issues with sediment sample processing. As described previously and discussed in detail by Goff et al. (2008), the laboratory-based analyses used to generate the usSEABED extracted data often exclude hard components like shell and gravel and may therefore introduce a bias toward finer particles. Goff et al. (2008) found that a simple correction (subtracting 0.5 φ from extracted data) removed the average bias between extracted and parsed mean grain size datasets. We used that bias correction, but note that it may not apply equally across the whole study area or all time periods and surveys. The model could still have under-predicted coarse sediments in some areas dominated by extracted data. Moreover, even parsed data may exhibit a bias against very large grains (especially cobbles and boulders) if they were excluded by mechanical sampling devices or removed in pre-processing. For the sediment composition models, we used both extracted and parsed datasets without applying any bias correction to account for the exclusion of hard components in the extracted data. As a result, the models were likely biased toward finer particles and may under-predict the fraction of gravel particles.

Other issues arise from the long time span over which samples were collected. Samples in the usSEABED database were collected over multiple decades, and thus variability in grain size and sediment composition data likely includes a temporal component in addition to spatial variability. It is possible that a sample collected in 1970 no longer reflects the true state of the seafloor, but it was used in the model as such. Also, positional uncertainty for survey locations was considerably greater for data collected decades ago.

Mean grain size is a suitable measure of sediment character at survey sites where sediment composition has a unimodal distribution, since mean grain size will represent the typical size of sediment particles in the sample. However, if the distribution of sediments in a sample is bimodal or multi-modal, then mean grain size will not indicate the typical size of sediment particles at the survey site (and in fact very few particles in the sample may be this size). For example, the mean grain size for a sample of gravelly-mud sediments could correspond to sand, even though sand may not be part of the sample. The mud, sand, and gravel fraction models can be used conjunction with the mean grain size models to mitigate this limitation.

Given that previous maps of sediment composition consisted of point data depicting the dominant sediment type at each location (e.g, Williams et al., 2006), the maps developed here represent a considerable advance over previously available information. However, given the limitations associated with the use of the usSEABED

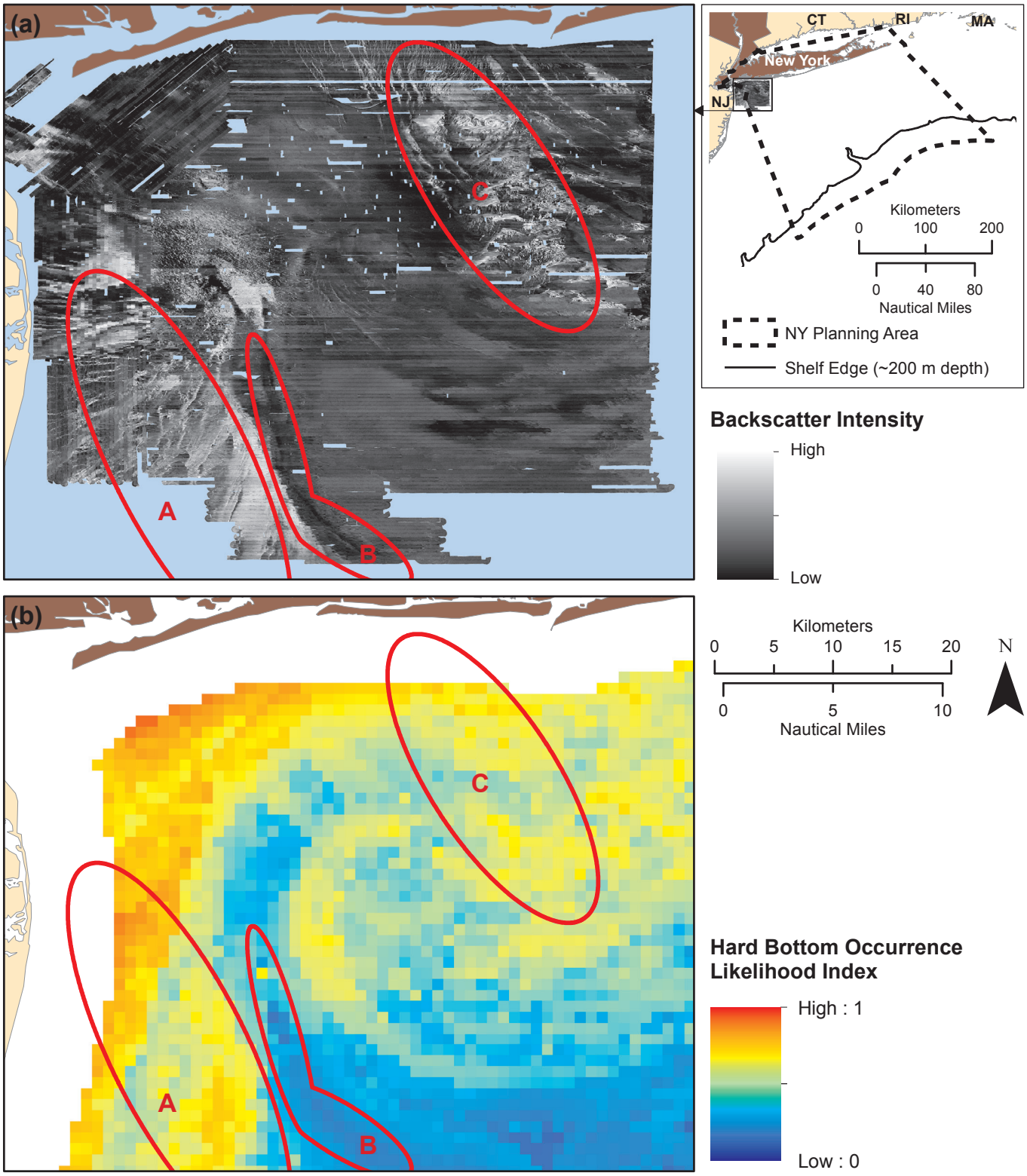

Figure 3.14. Comparison of overlapping portions of the (a) USGS acoustic backscatter data (from Schwab et al., 2002) and (b) the predicted hard bottom occurrence likelihood index. Higher backscatter intensity indicates coarser sediments (e.g., gravel) while lower backscatter intensity indicates finer sediments (e.g., sand and mud). Hard bottom data courtesy of USGS usSEABED database, NOS Hydrographic database (NOAA NGDC 2011), and The Nature Conservancy (Greene et al., 2010; J. Greene, The Nature Conservancy, personal communication, March, 2011; M. Fogarty, NMFS, personal communication, March, 2011).

sediment data, the maps of predicted mean grain size and sediment composition fractions should be used primarily to describe general patterns in sediment distribution. Maps of model uncertainty can be used to identify areas where additional survey data are needed and for risk analyses related to decision-making under uncertainty.

Hard Bottom Occurrence Model

The MaxEnt model of the likelihood of hard bottom occurrence performed well in the cross-validation ROC-like analysis. However, there are a number of limitations to the interpretation of this presence-only model, and it should be considered an experimental product.

First, the environmental predictor variables used to characterize hard bottom locations were at a considerably coarser spatial resolution than most hard bottom features on the seafloor (e.g., individual boulders, patches of exposed bedrock). As a result, the value associated with a given hard bottom point for a predictor may misrepresent the actual value at that precise location. Finer-scale environmental predictor data would enable the model to characterize hard bottom locations more accurately in terms of the environmental predictors, and as a result model predictions would be more reliable.

Second, MaxEnt solutions using presence-only data require that sampling effort is distributed homogenously over the study area or that biases are known and integrated into the model. We know that sampling effort was heterogeneously distributed and that there were significantly more samples collected close to shore, but we don't know exactly how effort is distributed. Because we were concerned about sample bias we excluded a large number of hard bottom locations in nearshore areas. Sample bias can result in model predictions that are overfit to more densely surveyed areas (Phillips et al., 2009; Elith et al., 2011). Because of limitations related to sample bias and the inability of MaxEnt models to identify prevalence, Elith et al. (2011) suggest that presence-absence modeling methods should be used if presence-absence survey data is available. However, reliable hard bottom absence data was not available in the study area.

Third, unlike the mean grain size and sediment composition models, the MaxEnt output did not provide a spatial map of prediction uncertainties. Therefore, it was not possible to assess changes in prediction certainty associated with the location of input data or its variability. Lastly, the model did not provide any indication of the size of predicted hard bottom features. Rather, the model provided only an indication of the likelihood of at least one hard bottom point sample occurring at a given location. This, of course, depends on sample effort – but as previously noted the heterogeneity in effort is not explicitly included in the model.

Additional fundamental limitations to models developed from presence-only data are discussed in detail by Elith et al. (2011); anyone interested in quantitative application of the hard bottom model results should thoroughly read and understand the limitations discussed in that article.

Previous maps of hard bottom locations in the study area consisted of point data depicting survey locations where hard bottom features were observed, with no indication of the relative likelihood of occurrence across the study area (Greene et al., 2010). Therefore, in spite of the limitations associated with presence-only modeling, the model of hard bottom occurrence developed here provides additional information at unsampled locations that has previously been unavailable, and may be useful to spatial planning until detailed hard bottom distribution data can be collected.

3.6. ACKNOWLEDGMENTS

We thank Jenn Greene and Mark Anderson (The Nature Conservancy) and Michael Fogarty (NMFS) for providing hard bottom point data used by Greene et al. (2010) in the Northwest Atlantic Ecoregional Assessment and John Goff (University of Texas at Austin) for providing surficial sediment grain size data. Bryan Costa, Will Sautter, and Timothy Battista of the NOAA Biogeography Branch provided helpful discussions in support of this work and also assisted with data acquisition/analysis for bathymetry and vector shorelines. John Goff and Brian Calder provided detailed reviews that improved an earlier version of this chapter. However, any errors or omissions are the sole responsibility of the authors.

3.7. REFERENCES

Allen, J.S., R.C. Beardsley, J.O. Blanton, W.C. Boicourt, B. Butman, L.K. Coachman, A. Huyer, T.H. Kinder, T.C. Royer, J.D. Schumacher, R.L. Smith, and W. Strurges. 1983. Physical oceanography of continental shelves. Rev. Geophys. Space Phys. 21:1149-1181.

Brown, C.J., B.J. Todd, V.E. Kostylev, and R.A. Pickrill. 2011. Image-based classification of multibeam sonar backscatter data for objective surficial sediment mapping of Georges Bank, Canada. Continental Shelf Research 31:S110-S119.

Butman, B., T.J. Middleton, E.R. Theiler, and W.C. Schwab. 2003. Topography, shaded relief and backscatter intensity of the Hudson Shelf Valley, offshore of New York: U.S. Geological Survey Open-File Report 03-372. http://pubs.usgs.gov/of/2003/of03-372/.

Butman, B., D.C. Twichell, P.A. Rona, B.E. Tucholke, T.J. Middleton, and J.M. Robb. 2006. Sea floor topography and backscatter intensity of the Hudson Canyon region offshore of New York and New Jersey: U.S. Geological Survey Open-File Report 2004-1441, version 2.0. http://pubs.usgs.gov/of/2004/1441/.

Cressie, N.A.C. 1993. Statistics for spatial data (revised ed.). New York: John Wiley & Sons, Inc.

De Falco, G., R. Tonielli, G. Di Martino, S. Innangi, S. Simeone, and I.M. Parnum. 2010. Relationships between multibeam backscatter, sediment grain size, and Posidonia oceanica seagrass distribution. Continental Shelf Research 30:1941-1950.

Deutsch, C.V. and A.G. Journel. 1998. GSLIB: Geostatistical software library and user's guide (second ed.). New York: Oxford University Press.

Elith, J., C.H. Graham, R.P. Anderson, M. Dudı´k, S. Ferrier, A. Guisan, R.J. Hijmans, F. Huettmann, J.R. Leathwick, A. Lehmann, J. Li, L.G. Lohmann, B.A. Loiselle, G. Manion, C. Moritz, M. Nakamura, Y. Nakazawa, J. M. Overton, A.T. Peterson, S.J. Phillips, K.S. Richardson, R. Scachetti-Pereira, R.E. Schapire, J. Sobero´n, S. Williams, M.S. Wisz, and N.E. Zimmermann. 2006. Novel methods improve prediction of species' distributions from occurrence data. Ecography 29:129-151.

Elith, J., S.J. Phillips, T. Hastie, M. Dudik, Y.E. Chee and C.J. Yates. 2011. A statistical explanation of MaxEnt for ecologists. Diversity and Distributions 17:43–57.

Environmental Systems Research Institute, Inc. (ESRI). 2011a. ArcGIS Desktop: Release 10. Redlands, CA: Environmental Systems Research Institute.

Environmental Systems Research Institute, Inc. (ESRI). 2011b. ArcGIS Desktop 10 Resource Center. Cross Validation (Geostatistical Analyst). URL: http:/help.arcgis.com/en/arcgisdesktop/10.0/help/index.html#//00300000000z000000.htm.

Ferrini, V.L. and R.D. Flood. 2006. The effects of fine-scale surface roughness and grain size on 300 kHz multibeam backscatter intensity in sandy marine sedimentary environments. Marine Geology 228:153-172.

Fielding, A.H. and J.F. Bell. 1997. A review of methods for the assessment of prediction errors in conservation presence/absence models. Environmental Conservation 24:38-49.

Fogarty, Michael. 2011. NOAA National Marine Fisheries Service (NMFS). Northeast Fisheries Science Center. Personal communication.

Folk, R.L. 1954. The distinction between grain size and mineral composition in sedimentary rock nomenclature. Journal of Geology 62:344-359.

Folk, R.L. 1974. The petrology of sedimentary rocks. Austin, TX: Hemphill Publishing Co. 182 pp.

Goff, J.A. 2011. University of Texas at Austin. Personal communication.

Goff, J.A., C.J. Jenkins, and B. Calder. 2006. Maximum likelihood resampling of noisy, spatially correlated data. Geochemistry, Geophysics, and Geosystems 7, Q08003, doi:10.1029/2006GC001297.

Goff, J.A., C.J. Jenkins, and S.J. Williams. 2008. Seabed mapping and characterization of sediment variability using the usSEABED data base. Continential Shelf Research 28:614-633.

Golub, G.H. and C.F. Van Loan. 1996. Matrix Computations, 3rd edition. Johns Hopkins University Press.

Goovaerts, P. 1997. Geostatistics for natural resources evaluation. New York: Oxford University Press.

Greene, J.K. 2011. The Nature Conservancy. Eastern U.S. Division. Personal Communication.

Greene, J.K., M.G. Anderson, J. Odell, and N. Steinberg, eds. 2010. The Northwest Atlantic Marine Ecoregional Assessment: Species, Habitats and Ecosystems. Phase One. The Nature Conservancy, Eastern U.S. Division, Boston, MA. URL: http://www.nature.org/ourinitiatives/regions/northamerica/areas/easternusmarine/explore/index.htm.

Harris, B.P. and K.D.E. Stokesbury. 2010. The spatial structure of local surficial sediment characteristics on Georges Bank, USA. Continental Shelf Research 30:1840-1853.

Krumbein, W.C. and L.L. Slass. 1963. Stratigraphy and sedimentation. San Francisco: W.H. Freeman. 660 pp.

Lathrop, R.G., M. Cole, N. Senyk, and B. Butman. 2006. Seafloor habitat mapping of the New York Bight incorporating sidescan sonar data. Estuarine, Coastal and Shelf Science 68:221-230.

National Oceanic and Atmospheric Administration (NOAA) National Geophysical Data Center (NGDC). 2011. NOAA National Ocean Service (NOS) and U.S. Coast and Geodetic Survey (USCGS) Bottom Type Descriptions from Hydrographic Surveys. NGDC Data Set G10163. Online database. http://www.ngdc.noaa.gov/geosamples/survey.jsp. Accessed June 29, 2011.

Peterson, A.T., M. Papes, and M. Eaton. 2007. Transferability and model evaluation in ecological niche modeling: a comparison of GARP and Maxent. Ecography 30:550-560.

Phillips, S.J., R.P. Anderson, and R.E. Schapire. 2006. Maximum entropy modeling of species geographic distributions. Ecological Modelling 190:231-259.

Phillips, S.J. and M. Dudik. 2008. Modeling of species distributions with Maxent: new extensions and a comprehensive evaluation. Ecography 31:161-175.

Phillips, S.J., M. Dudik, J. Elith, C.H. Graham, A. Lehmann, J. Leathwick, and S. Ferrier. 2009. Sample selection bias and presence-only distribution models: implications for background and pseudo-absence data. Ecological Applications 19:181–197.

Poppe, L.J., J.S. Schlee, and H.J. Knebel. 1994. Map showing distribution of surficial sediment on the Mid-Atlantic continental margin, Cape Cod to Albemarle Sound. USGS. USGS United States Geological Survey (US Department of the Interior). Misc. Invest. Sen, Map I-1987-D.

Poppe, L.J., S.J. Williams, and V.F. Paskevich. 2005. U.S. Geological Survey East-Coast Sediment Analysis: Procedures, Database, and GIS Data: Open-File Report 2005-1001, U.S. Geological Survey, Coastal and Marine Geology Program, Woods Hole Science Center, Woods Hole, MA.

Reid, J.M., J.A. Reid, C.J. Jenkins, M.E. Hastings, S.J. Williams, and L.J. Poppe. 2005. usSEABED: Atlantic coast offshore surficial sediment data release: U.S. Geological Survey Data Series 118, version 1.0. http://pubs.usgs.gov/ds/2005/118/.

Schwab, W.C., J.F. Denny, B. Butman, W.W. Danforth, D.S. Foster, B.A. Swift, L.L. Lotto, M.A. Allison, and E.R. Thieler. 2000. Seafloor characterization offshore of the New York-New Jersey metropolitan area using sidescan-sonar: U.S. Geological Survey Open-File Report 00-295. http:// pubs.usgs.gov/of/2000/of00-295.

Schwab, W.C., J.F. Denny, D.S. Foster, L.L. Lotto, M.A. Allison, E. Uchupi, W.W. Danforth, B.A. Swift, E.R. Thieler, and B. Butman. 2002. High resolution quaternary seismic stratigraphy of the New York Bight continental shelf: U.S. Geological Survey Open-File Report 02-152. http:// pubs.usgs.gov/of/2002/of02-152/.

Wentworth, C.K. 1922. A scale of grade and class terms for elastic sediments. The Journal of Geology 30:377-392.

Williams, S.J., M.A. Arsenault, L.J. Poppe, J.A. Reid, J.M. Reid, and C.J. Jenkins. 2006. Surficial sediment character of the New York-New Jersey offshore continental shelf region: a GIS compilation. U.S. Geological Survey Open- File Report 2006-1046. Online at http://pubs.usgs.gov/of/2006/1046.